

UVM ScholarWorks

Multi-Scale Assessment of Gully Erosion at Road Drainage Outlets

Item Type	thesis;article
Authors	Estabrook, Emma Louise
Download date	2026-06-05 22:13:01
Link to Item	https://hdl.handle.net/20.500.14849/3454

MULTI-SCALE ASSESSMENT OF GULLY EROSION AT ROAD DRAINAGE
OUTLETS

A Thesis Presented

by

Emma Estabrook

to

The Faculty of the Graduate College

of

The University of Vermont

In Partial Fulfillment of the Requirements
for the Degree of Master of Science
Specializing in Natural Resources

May, 2022

Defense Date: December 10, 2021

Thesis Examination Committee:

Beverley Wemple, Ph.D., Advisor

Mandar Dewoolkar, Ph.D., Chairperson

Breck Bowden, Ph.D.

Scott Hamshaw, Ph.D.

Cynthia J. Forehand, Ph.D., Dean of the Graduate College

ABSTRACT

Gully erosion and sediment deposition from roads are underrated sources of sediments entering receiving waterways. While gully erosion has been studied throughout the world, the monitoring of the temporal and spatial erosional processes related to culverts and road drainage is rare. The objectives of this study are to quantify rates of gully erosion from Vermont's transportation drainage networks at multiple temporal scales and report on insights gained from a multi-scale approach to monitoring gully erosion. To quantify event to seasonal timescales of gully erosion, high resolution terrestrial LiDAR surveys were conducted at 13 field sites. Field sites were monitored at least seasonally from September 2019 to May 2021. To evaluate longer-term rates of gully erosion, a coarser approach was implemented that used high resolution airborne LiDAR that covered a longer time interval than field surveys allowed. Culvert outlet locations were inspected for evidence of gully erosion and a sample of gully volume change was estimated via digital elevation model of difference. Results of this study indicate that gullies at road drainage outfalls are a common occurrence in our study region with a median gully frequency of one in every 2 kilometers of road. Gully presence is influenced by road length, elevation, and slope steepness, revealed by different scales of analysis. Estimates of gully change ranged $-24 \text{ m}^3/\text{year}$ to $269 \text{ m}^3/\text{year}$ with 76% of features examined eroding less than $10 \text{ m}^3/\text{year}$. These features appear to be dynamically evolving, with some evidence that gully stabilization occurs in some sites over time. Gully stabilization may be achieved over time as these features reach an equilibrium slope or when grade controls such as fallen trees arrest incision. This study can be used as a building block for making roads more resilient to extreme weather events and reducing the environmental impact of roads.

ACKNOWLEDGEMENTS

Vermont Agency of Transportation funded my graduate studies and research.

University of Vermont Spatial Analysis Lab partially funded my research.

Beverly Wemple served as my advisor for my studies. I would not have been able to complete this thesis without her help.

Mandar Dewoolkar served on my thesis committee as the Chairperson.

Breck Bowden served on my thesis committee and as my undergraduate academic advisor.

Scott Hamshaw served on my thesis committee. He also trained me to use the terrestrial LiDAR scanner and GPS equipment. He also assisted me with the workflow of the airborne LiDAR gully volume estimation.

Frank Piasecki helped me set up the VTrans project and with LiDAR field work.

Luc Burnier assisted me with the LiDAR field work. He also helped with the gully identification and volume change estimations.

Jake Campbell created a python script to measure road lengths and assisted with gully identification and volume change.

Carly Alpert, Chris Carlos, Kathryn Koberna, and Emma Parks, assisted with the gully identification and volume change.

Members of the Technical Advisory Committee, thank you for providing helpful feedback to me during this project. I hope my contributions can help the state with TMDL planning.

TABLE OF CONTENTS

	Page
ACKNOWLEDGEMENTS	ii
LIST OF TABLES	vi
LIST OF FIGURES	viii
CHAPTER 1: INTRODUCTION	1
CHAPTER 2: LITERATURE REVIEW	3
2.1 Geomorphic & Water Quality Impacts from Roads	3
2.2 Gully Erosion	4
2.4 Channel Morphology, Dynamics, and Control	6
2.5 Methodological Approaches to Investigate Gully Erosion	8
2.6 Local Context of Vermont and Lake Champlain	10
2.7 Summary	12
CHAPTER 3: MULTI-SCALE ANALYSIS OF GULLY EROSION WITHIN ROAD SETTINGS	13
3.1 Introduction	13
3.2 Methodology	16
3.2.1 Study Area	16
3.2.2 Extensive gully monitoring using GIS and airborne LiDAR data	18
3.2.3 Intensive Gully Monitoring using Terrestrial LiDAR Surveys	22

Terrestrial LiDAR Surveys	22
3.2.4 Data Analysis.....	24
3.3 Results.....	31
3.3.1 Extensive Airborne Surveys	31
3.3.2 Intensive Terrestrial LiDAR Surveys.....	39
3.4 Discussion	48
3.5 Conclusions	51
CHAPTER 4: GULLY EROSION AND PHOSPHORUS PRODUCTION.....	53
4.1 Introduction	53
4.2 Methods.....	53
4.3 Findings.....	57
CHAPTER 5: CONCLUSIONS, REFLECTION AND FUTURE WORK	62
5.1 Informing Policy.....	62
5.2 Methodological Insights and Challenges	64
LITERATURE CITED.....	68

LIST OF TABLES

Table	Page
Table 1. Quality level, acquisition dates and pixel resolution for airborne LiDAR data used for this study. All LiDAR data accessed from the Vermont Geodata Portal at https://geodata.vermont.gov/	19
Table 2. Description of variables used for study. There were two response variables: gully occurrence and gully volume change. Gully occurrence was used only for the airborne LiDAR analysis and volume change was analyzed for both the airborne LiDAR and terrestrial LiDAR surveys. The explanatory variables included topographic conditions, physical conditions, and temporal conditions. The asterisk at the bottom of the table indicates if a variable was used for only one of the analyses.	27
Table 3. Gully occurrence summaries by town. Some towns were only partially covered in the LiDAR extent and in turn only a small number of culverts were assessed. In cases where a town has less than 50 culverts, the percent of culverts with gullies and projected gully frequency were not calculated. Those towns are indicated by an asterisk.	32
Table 4. Uncertainty values associated with the estimates of gully change from the extensive airborne LiDAR work. Resolution of each DoD is also included.	39
Table 5. Summary statistics of each of the gullies surveyed. Metrics were calculated from the May 2020 surveys where sites were surveyed within a two-week period.	40
Table 6. Six of the terrestrial LiDAR survey sites were analyzed to assess the gully evolution stage and width/depth ratio. The gully evolution stage was determined by field observations, erosion rate, and morphological changes that occurred over the study period. Width/depth ratios were measured at each 2-meter cross section of the May 2020 survey round. The width and depth were measured from the lower bank of the side slopes to the lowest point in the gully. The width/depth ratio of each cross section was then summarized at the minimum, maximum, and mean ratio.	48
Table 7. Example of HUC12 subwatersheds covering the town of Barre, with total phosphorus (TP) loads extracted from the Clean Water Roadmap tool. Estimates were weighted for the percentage of town area in each HUC12 subwatershed and summed to generate an estimate of TP load by town.	57

Table 8: Case 1 - summaries for five selected towns used to generate estimates of phosphorus production from gullies and compare to phosphorus load extracted from the Vermont Clean Water Roadmap tool.....60

Table 9: Case 2 - summaries for two selected HUC12 subwatersheds used to generate estimates of phosphorus production from gullies and compare to phosphorus load extracted from the Vermont Clean Water Roadmap tool.61

LIST OF FIGURES

Figure		Page
Figure 1.	A conceptual model describing the spatial coverage and resolution afforded by modern topographic survey products (left) and the time scales and accuracy demands necessary to track topographic change (right panel). This framework informs the adoption of the multi-scale analysis of gullies in this study, drawing from multiple LiDAR-based products.	15
Figure 2.	Study area map of the airborne LiDAR and terrestrial LiDAR analysis. The left map is an extent map showing the study region for both the airborne LiDAR analysis (A) and terrestrial LiDAR surveys (B). Panel A shows the five time periods used to track gully occurrence and change using airborne LiDAR (with flight dates), gullies assessed for the analysis, and the impact zone of tropical storm Irene (see narrative). Panel B shows locations of 13 intensively monitored sites using terrestrial LiDAR surveys.	20
Figure 3.	Partial dependence plots of the seven best predictors of gully occurrence from the BRM model. Plots show how(?) gully occurrence depends on each predictor variable after accounting for the average effects of other predictors. The relative contribution of each predictor to the overall error reduction is shown as a percentage on the y axis. Rugs at the bottom of each plot show the distribution of data. The 3D model on the lower right shows the interaction between elevation and slope steepness in relation to gully occurrence.....	34
Figure 4.	Graphical description of each LiDAR time period collect showing the total monthly rainfall on the left and a histogram of gully volume change per year. For each geographical region, the proportion of months over 100 mm and over 200 mm was calculated in addition to the maximum total monthly rainfall. The gully volume change histograms show the median value for each time period on the dashed line. For the central region there are 5 gullies over 125 m ³ /year that are not plotted.	37
Figure 5.	Map showing the spatial distribution of gully volumes over the study area. Each airborne lidar time period is symbolized, and the impact zone of tropical storm Irene is shown. The size of points is based on the rate of gully change where smaller points are less change and larger points are more change. The estimated time periods of each geographic area are northeast 10/31/2005-11/9/2016, northwest 11/7/2008-11/15/2017, central 5/15/2009-11/15/2015, north central 5/15/2010-11/15/2017, and west central 12/7/2012-11/15/2017. ...	38

Figure 6. Gully volumes for May 2020 surveys vs. contributing road length (a), contributing road surface area (b), upslope contributing area (c), and slope steepness at culvert outfall (d). Road length, contributing road area, and contributing drainage area all had significant relationships to gully volume and the equation is listed on the graph. Slope steepness did not have a significant relationship to gully volume.....	41
Figure 7. Gully volume change over survey interval and the sum of rainfall to occur during that time. Although there is not a significant relationship between the sum of rainfall and volume change over survey interval. Visually, high rainfalls generally resulted in higher change.	43
Figure 8. Terrestrial LiDAR scanner derived geospatial products. Each map shows the gully feature of interest, cross sections taken every 2 m, location of culvert outlet, and direction of flow from the culvert. Letters A-F are associated to the cross-section plots in Figure 9. A: Digital elevation model of site 2 with 2-m cross sections. The culvert location is at cross section A, but the gully headcut is located above the culvert outlet. B: Digital elevation model of site 3 with 2 m cross sections. The outlet is in the upper right-hand corner of the figure with the flow of water from the culvert following the gully downslope. C: Digital elevation model of difference of site 31. This shows the elevation change that occurred between the first and last survey of the study period where red cells represent areas of erosion and blue cells represent deposition. The culvert outlet is located in the upper left-hand area of the figure and the flow of water follows the gully moving to the right. This site had woody debris about half way down the gully (symbolized as a black box) which splits this gully into two distinct reaches.....	44
Figure 9. Cross section plots of sites 2, 3, and 31. The label of each cross section is associated to the cross-section labels in Figure 6. The titles are also labeled describing the cross-section sample length. Cross sections A-C for site 31 were sampled before.....	46
Figure 10. Locations of culverts inspections to assess gully occurrence. Inset panels show selected areas for which gully volume areas were determined by DEM differencing.	55
Figure 11. Locations of culvert inspections conducted in GIS to assess gully occurrence (upper left panel, same dataset presented in Figure 10) and detailed maps for two HUC12 watershed where culvert assessments covered much of the watershed.....	56

CHAPTER 1: INTRODUCTION

Gully erosion is often overlooked, but sediment deposition via gully erosion can contribute significantly to a watershed's sediment budget (Poesen 2011, Katz et al. 2014b). Sediment from roads is often a less recognized source of pollutant entering receiving waterways. Roads alter flow paths which can lead to an extension of channels on previously unchanneled areas of the landscape (Montgomery 1994, Wemple et al. 1996, Galia et al. 2017). This has a variety of geomorphic impacts such as gully initiation and slope instability. In the short-term, transportation networks interrupt the flow regime and the movement of water and sediment between the channel and its floodplain. Over decades, transportation networks influence floodplain dynamics by stopping the meandering of channels across its floodplain (Blanton and Marcus 2009).

While gully erosion has been studied in South Africa, Ethiopia, California, and many other areas, monitoring of the temporal and spatial erosional processes related to culverts and road drainage is rare (Daba et al. 2003, Perroy et al. 2010, Seutloali et al. 2016, Galia et al. 2017). Although a preliminary attempt to quantify gully erosion and impact on phosphorus production in Vermont was completed by Piasecki (2020), the magnitude and rate of gully erosion is still largely unknown, given the relatively small number of gullies examined in his study. Wemple et al. (2017) also highlighted the importance of identifying severe erosion associated with road networks because it contributes an under-valued source of nutrient pollutant in the state. Further investigations are needed to understand the magnitude and impacts of concentrated outfall erosion from Vermont's roads. In this study

I investigated the timeframe that gully erosional processes are occurring on Vermont's roads. Specifically, with this research I asked:

1. How do rates of gully erosion vary at event, seasonal, and annual time scales within road settings in Vermont?
2. What additional morphological information emerge from a multi-scale approach to gully monitoring?

My motivation to conduct this research lies at the intersection of the built environment and natural resources. I am interested in how humans have influenced the surrounding environment over time and aspire to quantify these effects. Future development is inevitable, and it is extremely important we understand the impacts of road development. I hope this research can be used as a building block for the state to contribute to the goals of making Vermont's roads more resilient to extreme weather events and to reduce the environmental impact of our roads.

This thesis contains five chapters. This chapter serves as an overview and introduction to the document. Chapter 2 is a literature review which includes a narrative on impacts from roads, gully erosion, channel morphology, methodological approaches, and local context of Vermont. Chapter 3 contains the manuscript of my thesis research focused on the analysis of gully erosion at multiple scales. I intend to submit this chapter for publication in a peer reviewed journal. Chapter 4 contains an analysis of gully erosion and phosphorus production at the town and watershed level. Chapter 5 is a reflection on the challenges and impacts of my thesis research.

CHAPTER 2: LITERATURE REVIEW

2.1 Geomorphic & Water Quality Impacts from Roads

Roads and transportation infrastructure are ubiquitous landscape features with a range of environmental impacts (Forman et al. 2003). Roads can impact aquatic connectivity for fish and macroinvertebrates by blocking pathways between water bodies. Fine sediment and heavy metals entering streams from roads can decrease the water quality (Grayson et al. 1993). There is extensive literature on the impacts of roads on water quality (Jones et al. 2000, Croke and Mockler 2001, Blanton and Marcus 2009, Wemple et al. 2017).

Roads fundamentally change water flow by altering hillslope hydrology, which contributes to soil erosion. The presence of roads in steep environments alters the surface hydrology by concentrating run off which in turn changes the pathways of runoff and rearranges the drainage network of a site (Katz et al. 2014b). This concept is also described by Jones et al. (2000) where complex interactions can occur between road segments and flows of water especially in steep environments. In roadcut and fill embankments, water will flow into the roadcut embankment that needs to be drained through culverts. This changes the flow from diffused surface flow to concentrated flow downslope (Seutloali and Beckedahl 2015).

Roads alter flow paths which can lead to an extension of channels on previously unchanneled areas of the landscape. This has a variety of geomorphic impact such as gully initiation and slope instability. Erosion initiation is influenced by contributing area, slope steepness, rainfall intensity, and soil properties (Seutloali and Beckedahl 2015). The

conceptual model proposed by Jones et al. (2000) describes interactions between road and stream networks related with the natural physical networks (streams) and artificial networks (roads). The premise of this conceptual model was that roads alter the balance between the intensity of peak flows and the streams resistance to change (Jones et al. 2000). Montgomery (1994) also showed that geomorphic impacts of roads include destabilization of the surrounding hillslope, gullying and channelization, increased sediment load, and altered hydrology in receiving waters. Evidence of changes in bank erosion from upstream to downstream of a culvert has been reported. Road and stream connectivity can be increased from gully erosion. This makes gullies a potential sediment delivery pathway to receiving waterways.

2.2 Gully Erosion

A gully is often described as a defined channel on a hillslope that is eroded by concentrated water. A gully's cross sections can be rectangular or V-shaped and is cut into the soil over time (Bull and Kirkby 1997, Kirkby and Bracken 2009). They can also be defined as linear channels that are too large to be demolished by tillage equipment (USDA-SCS 1966). Rills and gullies are occasionally described interchangeably, but rills are often found on slopes between 2 and 12 degrees, while gullies are typically on steeper slopes with shallow soil depths. Gullies are diverse features throughout the world and many researchers have categorized gullies about their geographical region.

Gully erosion is one of the worst forms of erosion as it indicates extreme land degradation (Daba et al. 2003). The occurrence of gully erosion and exposed rock outcrop are indicators of severe soil erosion (Daba et al. 2003). This type of erosion is influenced

by elevation, slope, aspect, lithology, soil properties, storm events, and land use/land cover. Most gully systems occur on steep terrain (30%-50% slope) with a shallow soil depth (Daba et al. 2003). Katz et al. (Katz et al. 2014b) agreed that gullies are likely to occur in roads with steeper slopes and larger drainage areas. In addition to road contributing area and hillslope, Seutloali (2016) found that vegetation cover has a significant effect on the volumes of gullies along paved roads. Observations over time indicate that gully volumes typically increase through a widening and deepening rather than length increase (Hayas et al. 2019). Gully erosion processes are well understood in croplands, but less in other environments. It appears that much of the gullying related to urbanization occurs in developing countries (Poesen 2011). Although in general gullies are more likely to develop where urbanization increased the contributing area (Junior et al. 2010).

Sediment from roads is an underrated source of pollutant entering receiving waterways. Gully erosion is often overlooked, but sediment deposition via gully erosion can comprise of a large portion of a watershed's sediment budget (Poesen 2011, Katz et al. 2014b). Wemple et al. (2017) highlighted that road networks are often hydrologically connected to streams allowing a direct channel of pollutant movement from roads into receiving waterways. Many studies have focused on roads and their impact of degrading water quality through sediment mobilization, but it is necessary to accurately and effectively map and monitor gully erosion to understand the impacts of road networks on the soil and receiving waterways (Seutloali et al. 2016).

2.4 Channel Morphology, Dynamics, and Control

Gullies grow from processes within the gully that erode and remove materials at the headcut. The extension of the headcut occurs from overland flow, subsurface piping, and/or repeated mass movements (Kirkby and Bracken 2009). Gullies are formed by the concentrated flow of water that removes upland soil and parent material (USDA-SCS 1966). Gully growth occurs when the rate of erosion from water and erodibility of the soil are higher than the soil production and geomorphic processes in the area (Arabameri et al. 2018). Smith and Bretherton (1972) also state that instability occurs when the sediment transport from flowing water in a feature exceeds the sediment brought in by the flow (Bretherton 1972). A critical condition must be met for channel formation to occur which may be defined as a threshold that changes through a storm and as the channel develops over time (Bull and Kirkby 1997).

Slope stability reflects the balance of shear stress and strength of the earth material. Failures on hillslopes tend to occur once a rainfall exceeds an intensity threshold because when a soil becomes saturated its shear strength reduces (Bierman 2014). Rates of gully development (periods of erosion and periods of stability) may be influenced by the magnitude and frequency of storm event cycles. For hillslope incision to grow the rate of sediment transport out of a channel must exceed the rate of sediment entering the same location or channel infilling will occur. Erodibility is influenced by precipitation intensity, permeability of the soil, cohesiveness of the soil and vegetation (Bull and Kirkby 1997).

Streams and gullies are similar in the sense that they are both channel features. A channel is defined as a linear element that has indication of erosion and/or deposition from

flowing water (Bull and Kirkby 1997). Channel head can be defined as the farthest uphill location with well-defined banks (Montgomery and Dietrich 1988). Channels have a defined cross section that is distinguishable without flowing water and have recognizable banks. Channels have a wide variety of morphologies ranging from alluvial channels to incised V-shaped ephemeral channels (Bull and Kirkby 1997). The main difference between gullies and streams are that streams are controlled by fluvial processes with a consistent directional flow of water within the channel and gullies are mainly controlled by hillslope processes (Montgomery and Dietrich 1988). Erosional processes that control channel head locations are inversely related to contributing area and hillslope. For a given local slope and soil type, the contributing area required to initiate a channel is influenced by precipitation frequency, duration, and intensity. With this thought process, channel heads would advance upslope during wetter periods (Montgomery and Dietrich 1988). If a gully is hydrologically connected to a stream, the gully in theory would be the channel head to a stream. With Vermont likely to get wetter due to climate change, it is extremely important to understand where channel heads or gullies are likely to occur.

There are four main stages of gully development and evolution first proposed by Ireland et al. (Ireland et al. 1939, Schumm 1984). Stage 1 is the channel cutting stage where gully growth is slow. Stage 2 is characterized by the headward movement of nickpoints, caving of the gully walls, and deepening of the channel. Stage 2 has the most rapid gully growth and ends when erosion slows. Stage 3 is a period of healing where the slope of the gully walls are reduced, and plants begin to establish on the lowered slopes. Stage 4 is a period of stabilization, and it is characterized by the accumulation of new soil over the

gully channel. Changes in environmental conditions can cause stage 3 or 4 to revert to stage 2. A gully can have different morphologies throughout the feature (Ireland et al., 1939).

Katz et al (2014) found that gullies are likely to occur in roads that have steeper slopes and larger drainage areas. They also concluded that the existence of roads in steep environments alter the surface hydrology by concentrating run off which in turn shifts the pathways of runoff and reorganizes the drainage network (Katz et al. 2014b). Junior et al (2010) has also highlighted that gullies are more likely to develop where urbanization increases contributing areas (Junior et al. 2010).

2.5 Methodological Approaches to Investigate Gully Erosion

Rates of erosion quantified fieldwork are most detailed, but it is time consuming and difficult to analyze over a long period. Field methods such as erosion pins, silt fences, and topographic surveys can be used to document rates and volumes of soil erosion, but they range in accuracy (Ritter et al. 2002). Katz et al. (2014) studied gully erosion by measuring the widest, longest, and deepest location of the gully to measure volume change. Daba et al. (Daba et al. 2003) surveyed gullies in Ethiopia using photogrammetric techniques, GIS, and field measurements. The repeatability of the Terrestrial LiDAR Scanner (TLS) has been studied to quantify and separate 'true' and 'false' geomorphic change when using this technology to monitor gully change. It is supported as an accurate way to monitor change in gully erosion, but proper planning is necessary for best results in change detection. Castillo et al. (2012) agreed that TLS is an accurate field method to measure gully erosion, but it is an expensive and time-consuming field method. Finding

the best field method for gully erosion requires a balance of accuracy requirements and scale of the study area.

There are some limitations to measuring gullies in the field methods which includes uncertainty in extrapolating results to a larger area. Errors in the measured length, cross-sectional area, and volume can lead to overall inaccuracies in gully erosion estimates (Castillo et al. 2012). Volumetric surveys allow estimations of the soil volume lost, but actual soil loss is often underestimated (Seutloali and Beckedahl 2015). Perroy et al. (2010) compared gully volume estimates from TLS and airborne LiDAR to assess the accuracy at the landscape scale and found both methods underestimated gully volumes and cross-sectional areas, due to the point density at the bottom of the gully. This underestimation is due to the gully shapes (side walls and v-shaped cross section) which makes it difficult to acquire full coverage (Perroy et al. 2010). Field measurements provide the necessary data to understand erosion processes, but it is difficult to generalize to large areas due to complex interactions of erosion processes and site conditions (Seutloali and Beckedahl 2015).

Rates of erosion and gullies have also been successfully mapped and monitored using GIS and other remotely sensed data. GIS can analyze a larger sample size but is less accurate. Seutloali et al. (2016) investigated the feasibility of using readily available remotely sensed data to identify and assess gully erosion in South Africa. They found that gullies smaller than 50 m³ can only be accurately mapped when using very high spatial resolution data. This study did demonstrate that remotely sensed data can be used to aid in the mapping and assessing of road gully erosion (Seutloali et al. 2016). Hayas et al. (Hayas

et al. 2019) found that gully widths can be measured using imagery with a spatial resolution ranging from 0.5 – 1 m. Frankl (2013) agreed that the accuracy of gully mapping through remote sensing is dependent on the ability to detect gullies from aerial data. Other factors that influence accuracy is the horizontal accuracy of the data layers and errors in digitizing a gully network. Frankl et al. (2013) showed that their research proved to be useful for the analysis of change in gully volumes, although they made a distinction only between the low- and high-active gullies.

Multi-year LiDAR DEM comparisons provide more opportunity to document change over time compared to classic aerial imagery. A review of challenges in gully erosion research found that classic aerial photos do not often provide enough detail for gully monitoring, but airborne LiDAR is more feasible to monitor gully erosion through GIS (Poesen 2011). The main limitation of this analysis is the input data quality in relation to the gully sizes. These techniques need to be further developed and applied to a wide range of gullies (Poesen 2011).

Although field work and remote sensing techniques are useful tools to monitor gully channel development, there is a research need for longer data series with regular survey frequencies, control strategies, and standard methods related to gully erosion (Castillo and Gómez 2016). Gully erosion rates can vary greatly over time and not a single erosional process is applicable to all landscapes (Poesen 2011).

2.6 Local Context of Vermont and Lake Champlain

Lake Champlain has undergone tremendous changes in recent history (Smeltzer 2016). With the arrival of European settlers came deforestation and larger scale agriculture.

This clearing of the land eventually led to soil erosion and eutrophication of Lake Champlain. Eutrophication has led to cyanobacteria blooms in shallow portions of the lake. Vermont's first attempts to address these issues in Lake Champlain began in the 1960s in St. Albans Bay, but unfortunately the treatments installed were temporary and algal blooms continued (Winslow 2015). In the 1970s, Lake Champlain was the subject of scientific studies that estimated the first phosphorus loads to the lake and identified various potential sources. It was determined that the total phosphorus load to the lake at that time was 637 metric tons per year. During this time, there was growing scientific consensus that phosphorus was a key nutrient limiting algal growth in fresh water. This led the state to implement a Total Daily Maximum Daily Loads (TMDL) to limit the amount of phosphorus entering the lake. The building blocks of the TMDL were based on a set of in-lake phosphorus concentrations, total loading capacities for each lake segment, and an agreement of how reduction responsibilities were divided.

Phosphorus load estimations came from running a watershed model that was calibrated against phosphorus loads in rivers draining into Lake Champlain. The Soil and Water Assessment Tool (SWAT) was a major model used to identify maximum daily loads of phosphorus. SWAT is a basin-scale model that predicts the impacts of management on water and sediment yields. SWAT can model 1- to 100-year time periods and analyze pollutant contributions to sources (Tetra Tech 2015).

Roads fall within the developed land sources of phosphorus which includes roads, parking lots, lawns, athletic fields, buildings, and industrial facilities. Within the developed land sector, back roads are the largest source category in most lake segment due to roadside

ditches (E.P.A. 2016). Although the initial estimations for the TMDL took roads into consideration in a limited extent, gully erosion was not included in these estimations (E.P.A. 2016). There was research that went into establishing water quality standards for Lake Champlain, but it was limited in scope to the impact roads and the related erosion may contribute to phosphorus loading into Lake Champlain.

2.7 Summary

While gully erosion has been studied in South Africa, Ethiopia, California, and many other areas, monitoring of the temporal and spatial erosional processes related to culverts and road drainage is rare (Daba et al. 2003, Perroy et al. 2010, Seutloali et al. 2016, Galia et al. 2017). Although fieldwork and remote sensing techniques are useful tools to monitor gully channel development, there is a research need to combine historical techniques with detailed field measurements. Although a preliminary attempt to quantify gully erosion and impact on phosphorus production in Vermont was completed in 2020 (Piasecki 2020), the magnitude and rate of gully erosion was still largely unknown. Further investigations are needed to understand the magnitude and impacts of concentrated outfall erosion from Vermont's roads. This understanding is necessary for land use and climate change planning (Frankl et al. 2013).

CHAPTER 3: MULTI-SCALE ANALYSIS OF GULLY EROSION WITHIN ROAD SETTINGS

Emma Estabrook, Beverley Wemple, Scott Hamshaw, and Mandar Dewoolkar
In preparation for submission for publication

3.1 Introduction

Roads fundamentally change surface water flow by altering hillslope hydrology, which contributes to soil erosion and can lead to an extension of channels on previously unchanneled areas of the landscape (Montgomery 1994, Wemple et al. 1996, Katz et al. 2014b, Galia et al. 2017). The existence of roads in steep environments alters the hillslope hydrology by reducing infiltration rates, which in turn shifts the pathways of runoff and reorganizes the drainage network of the surrounding area (Katz et al. 2014a). This changes the flow from diffuse surface flow to concentrated flow downslope, with a variety of geomorphic impacts such as slope instability, erosion at drainage outfalls, and gully initiation (Seutloali and Beckedahl 2015).

Gullies are morphological features formed through fluvial erosion by concentrated runoff (Conforti et al. 2011, Arabameri et al. 2018). Roads can concentrate runoff and thus facilitate gully formation. Gully erosion increases connectivity between roads and streams making gullies a pathway for transfer of pollutants such as sediment, nutrients, and salt to receiving waterways. They typically form at steep headcuts, can extend hundreds of meters in a single storm, and can be difficult and costly to remediate (Kirkby and Bracken 2009). Mirroring the types of evolutionary changes observed in natural channels, gullies tend to go through predictable stages of evolution, as described by Schumm (1984), and observations of gullies over time indicate that their volumes

increase through stages of widening and deepening (Hayas et al. 2019). While gully erosion has been studied in South Africa, Ethiopia, California, and many other areas, temporal and spatial monitoring of erosional processes related to culverts and road drainage is rare.

A compilation of these studies by Poesen (2003) showed that rates of soil loss due to gully erosion varied widely by geographic setting, comprising as little as 10% of total soil loss in study sites in Europe to more than 70% in arid settings of California, USA, Australia, Spain, China and South Africa. Mass soil loss rates due to gully erosion ranging from 20-60% were common in study sites of humid settings in the eastern U.S. The prevalence of gully erosion and its contribution to downslope sediment transfer, especially to receiving waters, raises the importance of understanding this form of sediment and associated nutrient transport for mitigating soil loss and downstream water quality degradation.

Prior studies of gully erosion have employed a range of approaches to document gully occurrence, rates of change, and controls (Castillo and Gómez 2016). Rates of gully erosion can be quantified through a variety of field methodologies, including erosion pins, silt fences, and topographic surveys that range in accuracy (Ritter et al. 2002, Castillo et al. 2012) (Figure 1). Structure from motion (SfM) approaches via unmanned aircraft systems address some existing data-collection shortcomings, but are a problematic method due to obstruction by vegetation (Hamshaw et al. 2017). Advances in LiDAR technology allow monitoring landscape change quickly and overcoming other field methods limitations. It is now possible to visualize a gully as a digital surface model and with repeat surveys it is relatively easy to quantify change at specific locations of erosion and

deposition of the gully. LiDAR scanners are typically mounted on tripods (terrestrial LiDAR) or manned aircrafts (airborne LiDAR) (Bremer and Sass 2012). The use of terrestrial LiDAR scanning (TLS), in particular, is emerging as means of obtaining very high resolution (cm-scale) surface topography data, allowing for gully volume estimation and detection of rates of change through repeat surveys.

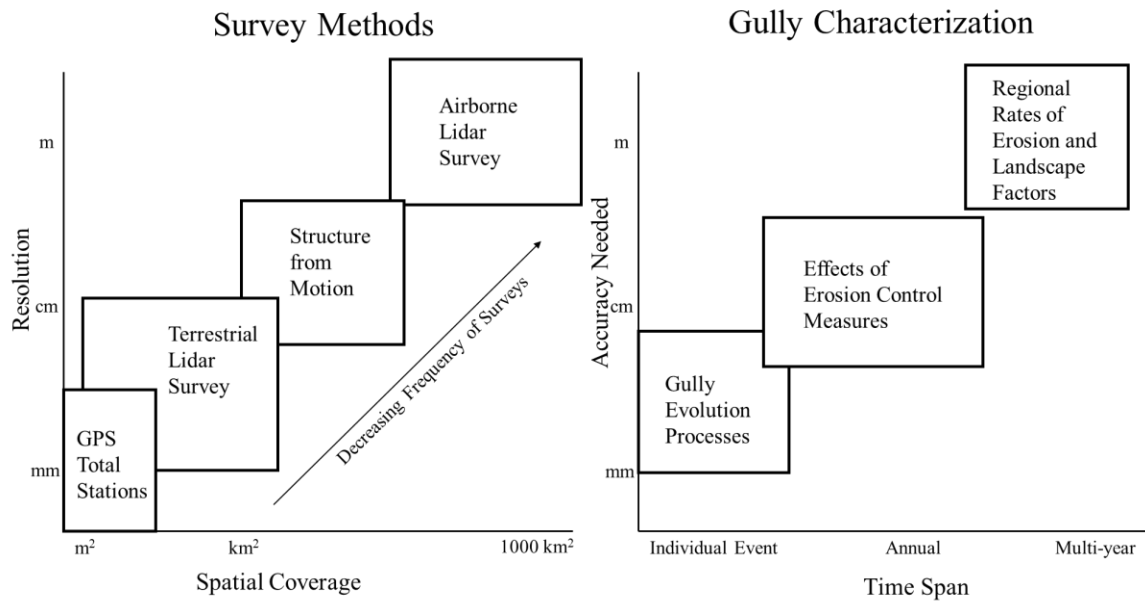


Figure 1. A conceptual model describing the spatial coverage and resolution afforded by modern topographic survey products (left) and the time scales and accuracy demands necessary to track topographic change (right panel). This framework informs the adoption of the multi-scale analysis of gullies in this study, drawing from multiple LiDAR-based products.

Gully erosion is a major driver of land degradation on the global scale and its impact cannot be underestimated as many countries are severely impacted by the magnitude of erosion rates (Castillo and Gómez 2016). In particular, further investigations are needed to understand the magnitude and impacts of gully erosion at road drainage

outfalls to aid in water quality remediation and climate adaptation planning (Frankl et al. 2013).

In this study, we leveraged LiDAR technologies to investigate the occurrence of gullying at road drainage outfalls in a mixed landcover setting of the northeastern U.S. (Figure 2). Using a combination of airborne and terrestrial LiDAR data products, we investigated the spatial distribution of gully occurrence at a broad spatial scale and estimated rates of gully erosion over multiple time scales. Our work was motivated by mandates to address water quality impairment caused by road-related erosion and leverages emerging geospatial technologies that are broadly available for application in other settings.

3.2 Methodology

Our study sites are situated in the northeastern U.S., within the state of Vermont, where a combination of rugged terrain, mixed land use, state, municipal and rural road networks create conditions that are conducive to water quality degradation (Wemple 2016). To examine gully occurrence using LiDAR technologies, we conducted inspections and analyses of road drainage outfalls using airborne LiDAR data, combined with repeated surveys using terrestrial LiDAR scanning at a set of 13 intensively monitored road drainage outfalls in Chittenden, Lamoille and Washington counties in northern Vermont.

3.2.1 Study Area

Vermont has a temperate climate with warm and humid summers and cold winters. Lake Champlain is the western border of the state with the Green Mountains extending in the north-south direction. Temperatures range from an average high of 75°F

(23.9°C) to 82°F (27.8°C) in the summer months and an average low of 2°F (-16.7°C) to 12°F (-11.1°C) in the winter. The annual precipitation ranges from about 889 mm in the Champlain valley and up to 1,524 mm in the mountains. The average snowfall ranges from 2,032 mm to 2,540 mm (<https://www.weather-us.com/en/vermont-usa-climate>). The last major geomorphic event was Tropical Storm Irene in 2011. The intensive survey sites are located within the Winooski and Lamoille River watersheds with both rivers eventually draining into Lake Champlain. The lake is an impaired water under the Clean Water Act with phosphorus (P) identified as an impairing pollutant (Mears and Martin 2016). The total maximum daily load (TMDL) for phosphorus, developed by the Environmental Protection Agency (EPA) in collaboration with the state of Vermont calls for reductions of P loading, including sediment-bound P delivered to receiving waters as a result of soil erosion (E.P.A. 2016). The largest source of phosphorus for Lake Champlain is derived from the agriculture sector. But developed land is the a near second as a source of phosphorus. Within the developed land sector, unpaved roads contribute P due to erosion and sedimentation from road surfaces and roadside ditches (USEPA, 2015). Statewide flooding, damage to infrastructure, and the delivery of nutrients and sediments to Lake Champlain during tropical storm Irene in 2011 has heightened attention and efforts to address the impacts of extreme storm events and road-related water quality degradation within the basin (Martin 2016, Wemple 2016).

3.2.2 Extensive gully monitoring using GIS and airborne LiDAR data

To understand regional patterns of gully erosion at road drainage outfalls, we used airborne LiDAR data from the Vermont's Quality Level 3 (QL3) collected between 2005-2012 and the Quality Level 2 (QL2) collected between 2013-2017. These acquisitions, focused on northern Vermont from Brandon (48.8234°N) to the Canadian border (Table 1, Figure 2). QL3 LiDAR has a vertical accuracy of less than or equal to 0.200 meters and QL2 is less than or equal to 0.100 meters (Heidemann 2012). Time periods of comparison for areas with multi-date collections ranged from 5 years (2012 to 2017) to 11 years (2005 to 2016) over the regions we assessed. We identified road drainage outfall locations using the VTrans Small Culvert Inventory available on the Vermont geodata portal (<https://geodata.vermont.gov/>) and the VTCulverts dataset compiled by the Vermont Agency of Transportation and made available at <https://vtculverts.org/>. To select representative towns for assessment, we conducted a GIS-based analysis using ArcGIS Pro v. 2.6 (ESRI, ©2020) of road grade and slope steepness. Slope steepness was estimated by resampling the 0.7 m resolution QL2 Slope (expressed as a percent value) raster obtained from the Vermont geodata portal to a 10-meter resolution to minimize local variation and extracted the slope value to each culvert point dataset. Road grade was estimated by extracting elevation from the statewide QL2 digital elevation model at 50-meter intervals for the entire road network within the study region, then using the difference in elevation along each 50 m road segment to determine the road grade. This percent grade was joined to each culvert point. We used these analyses to calculate the mean and median statewide road grade and outfall slope steepness values. Using these statewide summary

statistics, we selected 35 towns out of 242 towns in the state with outfall steepness and road grade values similar to the study region distribution, and with multi-date airborne LiDAR data coverage, for inspection of road drainage outfalls.

Table 1. Quality level, acquisition dates and pixel resolution for airborne LiDAR data used for this study. All LiDAR data accessed from the Vermont Geodata Portal at <https://geodata.vermont.gov/>.

Quality level	Collect Name/Year	Estimated acquisition date	Pixel resolution (m)
QL3	2005	October 31, 2005	1.0
QL3	2008	November 13, 2008	1.6
QL3	2009	May 15, 2009	1.0
QL3	2010	May 15, 2010	1.6
QL3	2012	December 6, 2012	1.6
QL2	Rutland, Northeast	November 13, 2013	0.7
QL2	Rutland, Middle East	May 15, 2014	0.7
QL2	Rutland, Middle West	November 4, 2014	0.7
QL2	Eastern VT, Lot 5	November 10, 2014	0.7
QL2	Eastern VT, Lot 6	May 15, 2015	0.7
QL2	Eastern VT, Lot 7	November 15, 2015	0.7
QL2	Windham County	November 10, 2015	0.7
QL2	Middle CT River	November 10, 2016	0.7
QL2	Western VT	November 15, 2017	0.7

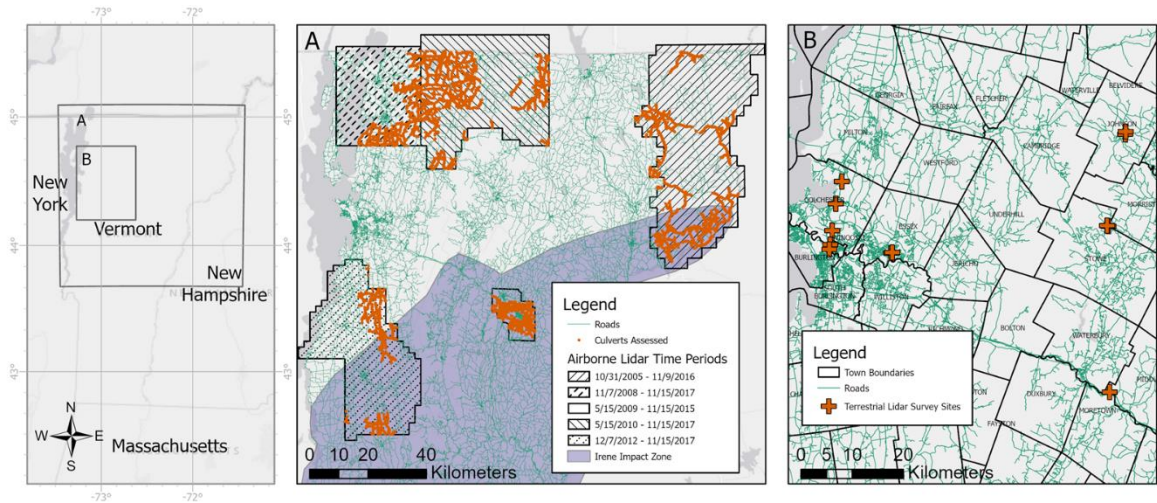


Figure 2. Study area map of the airborne LiDAR and terrestrial LiDAR analysis. The left map is an extent map showing the study region for both the airborne LiDAR analysis (A) and terrestrial LiDAR surveys (B). Panel A shows the five time periods used to track gully occurrence and change using airborne LiDAR (with flight dates), gullies assessed for the analysis, and the impact zone of tropical storm Irene (see narrative). Panel B shows locations of 13 intensively monitored sites using terrestrial LiDAR surveys.

Within each of the 35 selected study towns, for the extents covered by multi-date LiDAR, we conducted “heads up” inspections in a GIS environment of all culverts in the Small Culvert Inventory and VTCulverts datasets. This was done by zooming to each culvert point and visually inspecting for evidence of erosion near the culvert point location. Evidence of gully erosion was determined by a depression in the land, downslope of the culvert. If evidence of gully erosion was found, we coded a binary data field “gully” with the value 1. The “gully” field for all inspected culverts with no evidence of gulying was coded 0. For a randomly selected set of 303 gullies across the study region, we digitized the perimeter of the gullies to estimate change over time.

To estimate volume change between the two time periods for each DEM grid cell i , a DEM of Difference (DoD) was generated to assess change in elevation between two LiDAR surveys as

$$\text{DoDi} = \text{DEMi}_{T1} - \text{DEMi}_{T2} \quad (1)$$

where DEMi_{T1} is the elevation value for grid cell i in the first time period using LiDAR data from the QL3 collects, and DEMi_{T2} is the elevation value for grid cell i in second time period using LiDAR data from the QL2 collects. Positive values of DoD grid cells indicating a lowering of the surface from T1 to T2 (erosion) and negative values indicating elevation of the surface (deposition), for consistency in sign with our volume change estimates from the terrestrial LiDAR surveys.

The resulting DoD of each unique pair of collects was resampled to the resolution of DEM_{T1} which was the coarser resolution of the inputs. We then calculated the uncertainty and bias of the DoD to correct potential sources of error. The bias was estimated by digitizing a set of 25 to 30 reference polygons per QL3 collect in areas where we did not expect change to have occurred. We located these reference polygons in steep and flat areas including agricultural fields, parking lot surfaces, roadways, and urban settings to be representative of the collection area. We used zonal statistics to calculate the mean (and standard deviation) of the DoD for these reference polygons and designated the grand mean of these values as the bias (ϵ). Using the raster calculator, we then created a bias corrected DEM of Difference as follows

$$\text{DoDi}_{\text{corr}} = \text{DoDi} + 1.645 \epsilon \quad (2)$$

where 1.645ϵ approximates a 90% confidence interval correction and the error term ϵ may be positive or negative, which may raise or lower the corrected DoD surface to remove elevation bias associated with the two time periods compared.

With the bias corrected DoD, we calculated net volume change (Vchg) for each identified gully feature as

$$Vchg_{G_k} = \sum_{i=1}^N (DoDi_{corr} * Ni) * A \quad (3)$$

where N is the count of grid cells with elevation difference i within the digitized extent of each gully (G_k), $DoDi$ represents unique values of the vertical dimension of change, and A is the pixel resolution. We then expressed the volume change as an annual rate based on the date information in the LiDAR metadata.

3.2.3 Intensive Gully Monitoring using Terrestrial LiDAR Surveys

Terrestrial LiDAR Surveys

To understand gully evolution at the event time scale, we selected 13 sites for intensive monitoring at road drainage outfalls (Figure 2B). Site surveys began in the September 2019 on eight sites. Five more sites were added to the study in late fall 2019 and first surveyed in spring 2020. Surveys were conducted at least once each season (summer, fall, and spring following snowmelt) over the two-year study until July 2021 to assess gully change and quantify erosion rates. Each site was surveyed at least four times, with the highest frequency of surveying at sites 10 and 11 where we conducted 8 surveys over the two-year study period. Repeated surveys at all sites were used to quantify gully change over time.

Following site selection, we visually inspected each site, and established multiple scan positions, using 4-foot rebar stakes marked with reflective tape and survey caps to establish monumented tie points. Cylindrical reflectors were mounted on each tie point and raised to a height of 8 feet from the ground for surveying. To ensure coverage of the region

of active erosion, an area of interest for each gully was set at 3 times the gully width and 3 scan positions down the length of the gully. Surveys of the gully length were terminated when fencing or private property restrictions prevented access or when the gully feature entered a receiving stream. Tie point locations were set to ensure visibility from all scan positions along the elevation profile occupied by the gully.

Topographic data were acquired using a RIEGL VZ-1000 terrestrial LiDAR scanner at each scan position. A rugged field laptop with RiScan software was used for visual inspection of the resulting 3-dimensional point cloud in the field after each scan to ensure full coverage of the gully. Survey scans were processed using RIEGL software package RiScan Pro. This involved registering the raw 3D point clouds from the individual scans to a single scan. The 3D point cloud was edited to remove vegetation and anthropogenic features like culverts to create a 3D point cloud of the bare earth.

Calculating Gully Volume

The point cloud was edited using the built-in filtering tools and then manually edited in touch up areas. A touch up area was any area where the filtering tools did not filter out vegetation which was often on the gully side slopes. The bare earth point cloud was then exported to Applied Imagery Quick Terrain Modeler where a 0.1 m resolution DEM of the gully was generated using the adaptive triangulation fill method and spikes were filtered. To create a reference surface representative of a non-eroded/pre-gullying site condition we converted the first scan DEM to a TIN surface in Autodesk Civil 3D 2020 and then manually delineated the boundary of the gully as a 3-D polyline. We then created a baseline reference surface by interpolating inside the identified gully boundary with the

assumption that the land surface was a smooth surface. This baseline DEM and the LiDAR-scanned DEM were then compared in Quick Terrain Modeler to calculate the volume of each gully. The baseline DEM was used as the reference model to calculate feature volume for every subsequent survey over the monitoring time period. To quantify rates of gully erosion, we computed the difference in gully volume between survey dates.

3.2.4 Data Analysis

Airborne LiDAR Surveys

Calculation of Metrics

We estimated gully frequency along roads for each town assessed using our LiDAR data. In GIS, we determined the total length of road, the number of culverts assessed, and number of gullies identified. We then calculated the percent of culverts with gullies along inspected road segments and used this to estimate and the number of gullies per kilometer of road for the full road network.

We developed a set of possible independent variables to explain gully occurrence and rates of change using publicly available GIS data and GIS algorithms to derive variables (Table 2). Slope steepness at the culvert outfall was estimated by resampling the 0.7 m percentage slope raster to a 10-meter resolution to minimize local variation and using the Extract Values to Point geoprocessing tool to estimate the slope percentage at each gully location monitored. We used the 0.7 m resolution statewide LiDAR digital elevation model to extract elevation at culvert outfalls. We developed a Python script to estimate road length and road gradient draining to each culvert, using the culvert datasets to split the Vermont Road Centerlines data, conducting an iterative search within each segment for

a high point that exceeds the elevation of the segment culvert endpoints (and, if found, re-splitting the segment at the highpoint), and assigning the resulting segments to the lower elevation culvert on the segment. The Python script then computes road length and average slope for the segment(s) draining to each culvert. We used the Vermont Impervious Surfaces Land Cover 2016 dataset produced by the UVM Spatial Analysis Lab and VCGI for the Lake Champlain basin. Percent impervious surface was derived by generating a 100-meter buffer around each culvert and summarizing the area of impervious surface within each buffer. This metric was estimated to understand the representative land cover area in proximity to the culvert. Soil erodibility factor (Kw), parent material group, and hydrologic soil group for each culvert outfall were derived from the NRCS TOP20 Soils data. The parent material group was also recoded into three generalized groups: more erodible (glacial fluvial outwash, alluvial, and glaciolacustrine), less erodible (glacial till and dense till), and other (water, organic deposits, and miscellaneous units). The hydrologic soil group was also recoded into four more generalized groups: high drainage (A and B), low drainage (C and D), mixed (A/D, B/D, and C/D) and unknown (often used to indicate modern fill, urbanized at the time of the soil survey, quarries, water, etc.). Proximity to river was derived from the Vermont Agency of Natural Resources River Corridors centerlines dataset by buffering the river centerline by 200 m and coding all culverts within this buffer with a proximity flag. Culverts within the 2011 Tropical Storm Irene impact zone were derived by an overlay with the map extents of the region impacted by this 2011 storm documented in Castle *et al.*, (2013). We obtained precipitation totals between LiDAR surveys and airborne collects were obtained from airport weather stations

and the PRISM Climate Group (<https://prism.oregonstate.edu/>). The mean total monthly rainfall was estimated for each LiDAR collect. In addition, the maximum monthly rainfall, proportion of months over 150 mm, and proportion of months over 200 mm were calculated for each time period.

Table 2. Description of variables used for study. There were two response variables: gully occurrence and gully volume change. Gully occurrence was used only for the airborne LiDAR analysis and volume change was analyzed for both the airborne LiDAR and terrestrial LiDAR surveys. The explanatory variables included topographic conditions, physical conditions, and temporal conditions. The asterisk at the bottom of the table indicates if a variable was used for only one of the analyses.

Response Variables	
Gully Occurrence**	Culvert assessed with evidence of gully or no gully (yes/no)
Gully Volume Change	Gully volume change between LiDAR surveys (airborne and TLS) (m ³)
Explanatory Variables	
<i>Topographic Conditions</i>	
Slope Steepness	DEM-derived slope value at road outlet (%)
Elevation	DEM-derived elevation of culvert (m)
Road Grade	Average slope of road segments draining to culvert (%)
Road Length**	Length of road draining to culvert (m)
Road Area*	Surface area of road draining to culvert (m ²)
Contributing Area*	Draining area of upslope topography draining to culvert (m ²)
<i>Physical Conditions</i>	
Land Cover	Majority landcover within a 100-meter buffer of culvert. Coded as water, developed, barren, forest, shrub, agriculture, and wetland.
Percent Impervious	Percent impervious surfaces within a 100-meter buffer of culvert (%)
Soil Erodibility Factor	Susceptibility of a soil to erode by runoff and precipitation (kw)
Parent Material**	More and less erodible parent material
Hydrologic Soil Group**	Drainage of the soil by culvert. Coded as high and poor drainage.
<i>Temporal Conditions</i>	
Tropical Storm Irene Impact Zone**	Culvert located within impact zone of 2011 Tropical Storm Irene (yes/no)
Precipitation	Precipitation totals between LiDAR surveys (airborne and TLS) (mm)

*TLS analysis only

**Airborne LiDAR analysis only

Gully Presence Modeling

We used boosted regression trees (BRT) to evaluate gully occurrence from the airborne LiDAR dataset (n = 933). The goal of this analysis was to find variables that may be the best predictors of gully occurrence rather than creating an equation to estimate gully occurrence. BRTs are a machine learning approach that can estimate complex nonlinear relationships and compute interactions among predictor variables (Elith et al. 2008). We evaluated the best predictors of gully occurrence using the DISMO package in R following guidance from Elith et al. (2008). Tree complexity and learning rates were optimized during cross-validation. The best model had a tree complexity of 5 and a learning rate of 0.001 which produced 3,500 trees. The bag fraction was left at the default value of 0.5 meaning that at each iteration, 50% of the data were drawn from the full dataset. After initial model fitting, model simplification was performed to systematically drop predictors that contributed the least to total error prediction. This was done by removing the lowest relative importance variable of the model until every predictor had greater than 5% relative importance. We measured model performance using predictive deviance (goodness-of-fit) and the area under the receiver operator characteristic curve (AUC). The relative influence of predictors was determined by how often the predictor is selected to the model (Buston and Elith 2011).

Terrestrial LiDAR Surveys

We also developed a set of likely explanatory variables of gully size and rates of change for the intensively monitoring sites using publicly available GIS and precipitation data and data derivatives developed from these products (Table 2). Using the aerial

imagery, we measured road length and road surface area draining to each surveyed gully site using heads up digitizing in a GIS environment with a 0.7 m resolution digital elevation model to indicate slope breaks. The contributing upslope area draining to a site was determined by using 0.5 m contours (derived from 0.7 m digital elevation model) and visually delineating the drainage area. In urbanized areas with subsurface stormwater infrastructure, we used municipal stormwater collection system GIS data inventories to define areas draining to a site. We then used each of the inlets draining to a site as a pour point to visually delineate the drainage area using 0.5 m contours. Slope steepness was derived by the same methodology described above.

To assess variation in gully volumes collected from the terrestrial LiDAR surveys, we used gully volume from the May 2020 surveys, when all sites were surveyed within a two-week period. With this dataset, we examined the relationship of gully volume to road length, road surface area, contributing upslope area draining to the site, and slope steepness at the culvert outfall. We also used Natural Resources Conservation Service (NRCS) soils data to extract the soil erodibility factor and soil texture (quantified as a percent range of sand) for soil units at the culvert outfall and assessed these variables statistically against gully volume.

To assess the temporal variations in volume change, daily rainfall accumulation data for the period from September 2019 to May 2021 was acquired from the Burlington International Airport and Morrisville Airport. We summed the total rainfall to determine the accumulated rainfall between survey dates. We assessed temporal variation in gully erosion rates by examining the relationship between gully volume change and accumulated

rainfall between survey dates. We also created DoDs, using the approach described in section 3.2.2, from the high resolution terrestrial LiDAR surveys to evaluate where erosion and deposition occurred within the gully between surveys. Cross sections along the gully profile were also generated in Quick Terrain Modeler, situated every 2 meters from the gully headcut to end of area of interest (AOI) and the width of the cross sections were 5 - 10 meters. The width and depth of the gully was measured at each cross section to calculate the width/depth ratio throughout the gully length. This was done within Quick Terrain Modeler with the width and depth measured from the lower gully bank. For data visualization and statistical analysis, we used SPSS v. 27 and R v. 4. Statistically significant relationships were assessed at an alpha level of 0.05.

Using the DoDs, cross sections, erosion rates, and field observations, the gully evolution stage was characterized, following Ireland et. al (1939). Stage 1 is the channel cutting stage where gully growth is slow. Stage 2 is characterized by the headward movement of nickpoints, caving of the gully walls, and deepening of the channel. Stage 2 has the most rapid gully growth and ends when erosion slows. Stage 3 is a period of healing where the slope of the gully walls is reduced, and plants begin to establish on the lowered slopes. Stage 4 is a period of stabilization, and it is characterized by the accumulation of new soil over the gully channel. Changes in environmental conditions can cause stage 3 or 4 to revert to stage 2. A gully can have different morphology throughout the feature (Ireland et al., 1939).

3.3 Results

3.3.1 Extensive Airborne Surveys

Inspections of the multi-date airborne LiDAR imagery indicate that gully erosion is a common occurrence at culvert outfalls. Among the 9,823 culverts inspected, we identified 933 culverts with evidence of gully erosion, for a frequency of roughly one in every 10 culvert outfalls showing evidence of gulying (Table 3). Gully occurrence ranged from 2.5% to 25.4% at all culverts in the towns studied, with a mean of 12.4% and median of 11.0%. Estimated gully frequency extrapolated to town-level road networks ranged from 0.1 to 1.8 gullies per kilometer, with a median estimated frequency of one gully every two kilometers (i.e. 0.5 gully/km). Only three towns had an estimated frequency of more than 1 gully/km.

Table 3. Gully occurrence summaries by town. Some towns were only partially covered in the LiDAR extent and in turn only a small number of culverts were assessed. In cases where a town has less than 50 culverts, the percent of culverts with gullies and projected gully frequency were not calculated. Those towns are indicated by an asterisk.

Town	Total road length within town (km)	Road length within lidar collect (km)	Total culverts (#)	Culvert frequency (#/km)	Gullies at culvert outlets (#)	Percent of culverts with gullies (%)	Projected gully frequency (#/km)
Albany	122.1	13.7	56	4.08	11	19.6%	0.8
Barre Town	187.8	180.8	761	4.21	102	13.4%	0.6
Belvidere	43.3	9.4	67	7.13	17	25.4%	1.8
Berkshire	119.1	119.3	513	4.30	44	8.6%	0.4
Berlin	177.2	101.1	874	8.65	48	5.5%	0.5
Bloomfield	77.5	77.5	258	3.33	27	10.5%	0.3
Brandon	153.5	23.5	130	5.53	12	9.2%	0.5
Brighton	118.1	118.1	494	4.18	74	15.0%	0.6
Bristol	120.9	111.4	407	3.65	23	5.7%	0.2
Brunswick	22.2	22.2	127	5.71	14	11.0%	0.6
Burke	134.9	33.0	131	3.97	19	14.5%	0.6
Cambridge	210.3	61.4	239	3.89	23	9.6%	0.4
Charleston	124.8	20.8	103	4.95	15	14.6%	0.7
Concord	146.3	146.3	564	3.85	136	24.1%	0.9
Enosburgh	154.6	154.6	591	3.82	15	2.5%	0.1
Fairfax	177.8	52.6	298	5.67	20	6.7%	0.4
Fairfield	201.8	201.8	535	2.65	22	4.1%	0.1
Ferdinand*	66.1	66.1	32	0.48	2	*	*
Franklin	123.7	123.7	400	3.23	36	9.0%	0.3
Georgia	178.9	88.3	394	4.46	76	19.3%	0.9
Guidhall	49.9	49.9	209	4.19	24	11.5%	0.5
Hinesburg*	157.8	2.8	14	5.08	0	*	*
Leicester	65.4	65.4	195	2.98	28	14.4%	0.4
Lunenburg	128.0	128.0	639	4.99	37	5.8%	0.3
Monkton	118.1	118.1	304	2.57	19	6.3%	0.2
Newark	108.4	31.5	94	2.98	21	22.3%	0.7
Norton	34.1	34.1	246	7.21	60	24.4%	1.8
Orange*	97.6	0.3	2	6.93	0	*	*
Plainfield*	78.9	5.4	15	2.76	2	*	*
Sheldon	116.9	116.9	439	3.76	33	7.5%	0.3
Shoreham*	140.9	5.1	14	2.77	1	*	*
Starksboro*	118.7	1.6	9	5.75	2	*	*
Troy	105.4	79.4	418	5.27	41	9.8%	0.5

Victory	39.6	39.6	174	4.40	20	11.5%	0.5
Westfield	84.3	84.3	311	3.69	58	18.6%	0.7
Mean	117.3	71.1	287.3	4.4	30.9	12.4%	0.6
Median	119.1	65.4	246.0	4.2	22.0	11.0%	0.5
Min	22.2	0.3	2.0	0.5	0.0	2.5%	0.1
Max	210.3	201.8	874.0	8.6	136.0	25.4%	1.8

Boosted regression tree analysis revealed eight important predictors for gully occurrence along roads: elevation of culvert, slope steepness at culvert, percent impervious within 100 m buffer, road length draining to culvert, road grade draining to culvert, land cover, and maximum slope (Figure 3). We found that gully occurrence is more likely to occur at high elevations over 500 m than at lower elevations, on steeper slopes, and longer road segments as evidenced by the partial dependence plots. Forest, grass/shrub, and wetland land covers appear to have more gullies than other land covers. They indicate that gully occurrence fluctuates over percent imperviousness and road grade. Overall, gully occurrence is more likely at high road grade. There was one important interaction between predictors of gully occurrence. The relationship between culvert elevation and gully occurrence was dependent on slope steepness at culvert, with higher likelihood of gullying on slopes over 20% at elevations less than 200 m and greater than 500 m. The model explained 60.4% of the deviance using cross validation. The area under the receiver operating characteristics curve was 0.64 in cross validation correlation.

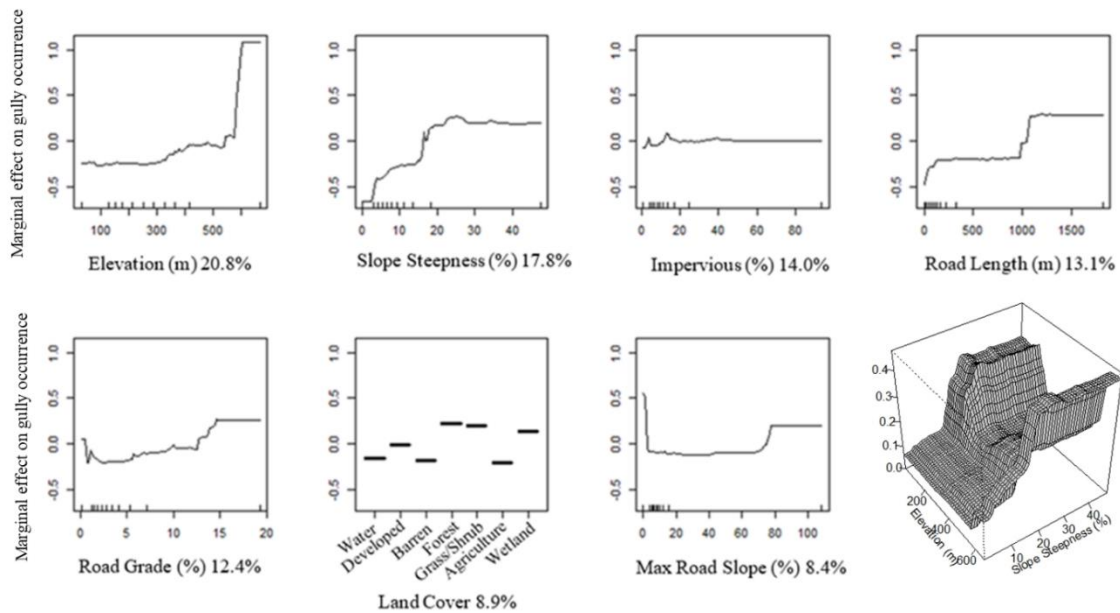


Figure 3. Partial dependence plots of the seven best predictors of gully occurrence from the BRM model. Plots show how(?) gully occurrence depends on each predictor variable after accounting for the average effects of other predictors. The relative contribution of each predictor to the overall error reduction is shown as a percentage on the y axis. Rugs at the bottom of each plot show the distribution of data. The 3D model on the lower right shows the interaction between elevation and slope steepness in relation to gully occurrence.

Estimates of gully change in time derived from the random sample of 303 gullies identified on the multi-date LiDAR, range from $-24 \text{ m}^3/\text{yr}$ to $269 \text{ m}^3/\text{yr}$ (Figure 4). Of the dataset, 69.3% of the gullies eroded more than $0.5 \text{ m}^3/\text{yr}$ and 17.5% of gullies deposited more than $0.5 \text{ m}^3/\text{yr}$. Although the dataset includes some cases of very high erosion over the compared time periods, 76% of features examined (230 of 303) eroded less than $10 \text{ m}^3/\text{yr}$. Overall, the largest gullies appear to occur near rivers or streams on roads that run parallel to the rivers. Every gully over $50 \text{ m}^3/\text{yr}$ had a Kw value over 0.4.

None of the explanatory variables examined were strong predictors of gully volumetric rate of change for the entire dataset but examining the datasets by geographic

area revealed complex controls on gully change. The median yearly erosion ranged from 0.5 m³/yr (Northeast) to 4.4 m³/yr (North central). Gullies detected in North central Vermont had the highest median change at ~4.5 m³/yr and had the highest proportion of monthly rainfall of over 150 mm. Central Vermont had the second highest median change per year. This area was impacted by the 2011 Tropical Storm Irene and contains the six largest gullies estimated with a maximum gully volume change of 268.5 m³/yr. The largest gully volume change is clustered in a 1500 m area along a highway that parallels Stevens Branch (a tributary to the Winooski River). These large gullies flowed directly into Stevens Branch and the slope steepness at these gullies all had slopes >20%. This area had the largest maximum monthly rain total of 281.5 mm. Northwest Vermont had the lowest median change per year at 0.5 m³/yr and it had the lowest maximum monthly rainfall. Only 1 gully in northwest Vermont was over 7.5m³/yr the largest gully had the highest kw factor of that collect at 0.49. Interestingly, North central Vermont has a much higher mean change despite being geographically close to Northwest collect. One reason for this difference may be that rainfall 2008 through 2010 was lower on average (determined by total monthly rainfall) and north central collect was in a higher elevation. Although 2012 to 2017 had the lowest proportion of months over 150- and 200-mm precipitation, it had the second highest maximum monthly rainfall of the collects. Within this collect, there are 8 gullies with over 20 m³/yr and four of them are clustered within a 1200-meter area directly draining to the New Haven River (three of them are clustered by one meander- almost looks like an Oxbow). The northeast region had the second lowest median gully change per year. Only

a portion of this collect was impacted by Irene, but every gully impacted by Irene had a change of over 10 m³/year.

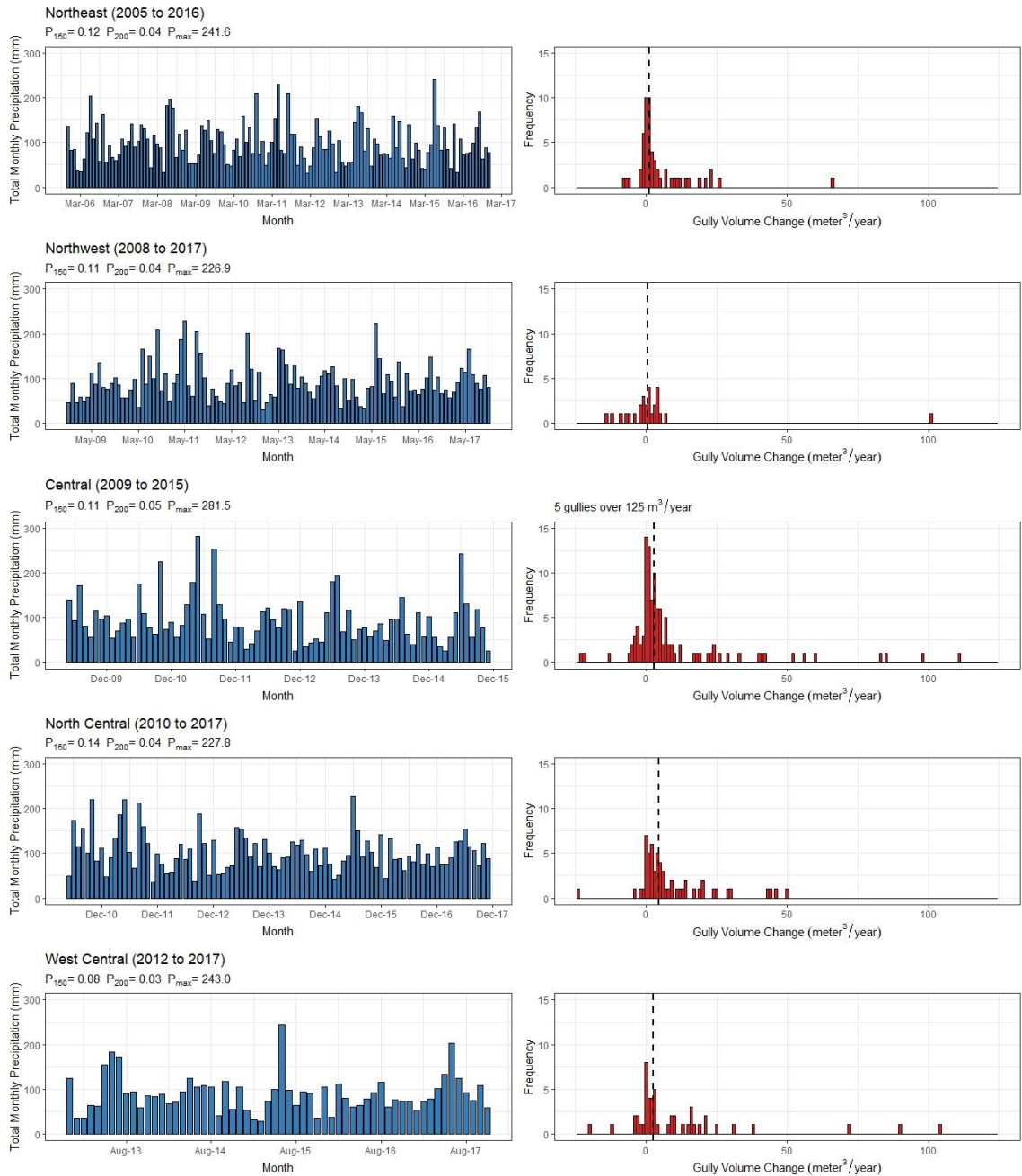


Figure 4. Graphical description of each LiDAR time period collect showing the total monthly rainfall on the left and a histogram of gully volume change per year. For each geographical region, the proportion of months over 100 mm (P_{100}) and over 200 mm (P_{200}) was calculated in addition to the maximum total monthly rainfall (P_{max}). The gully volume change histograms show the median value for each time period on the dashed line. For the central region there are 5 gullies over 125 m³/year that are not plotted.

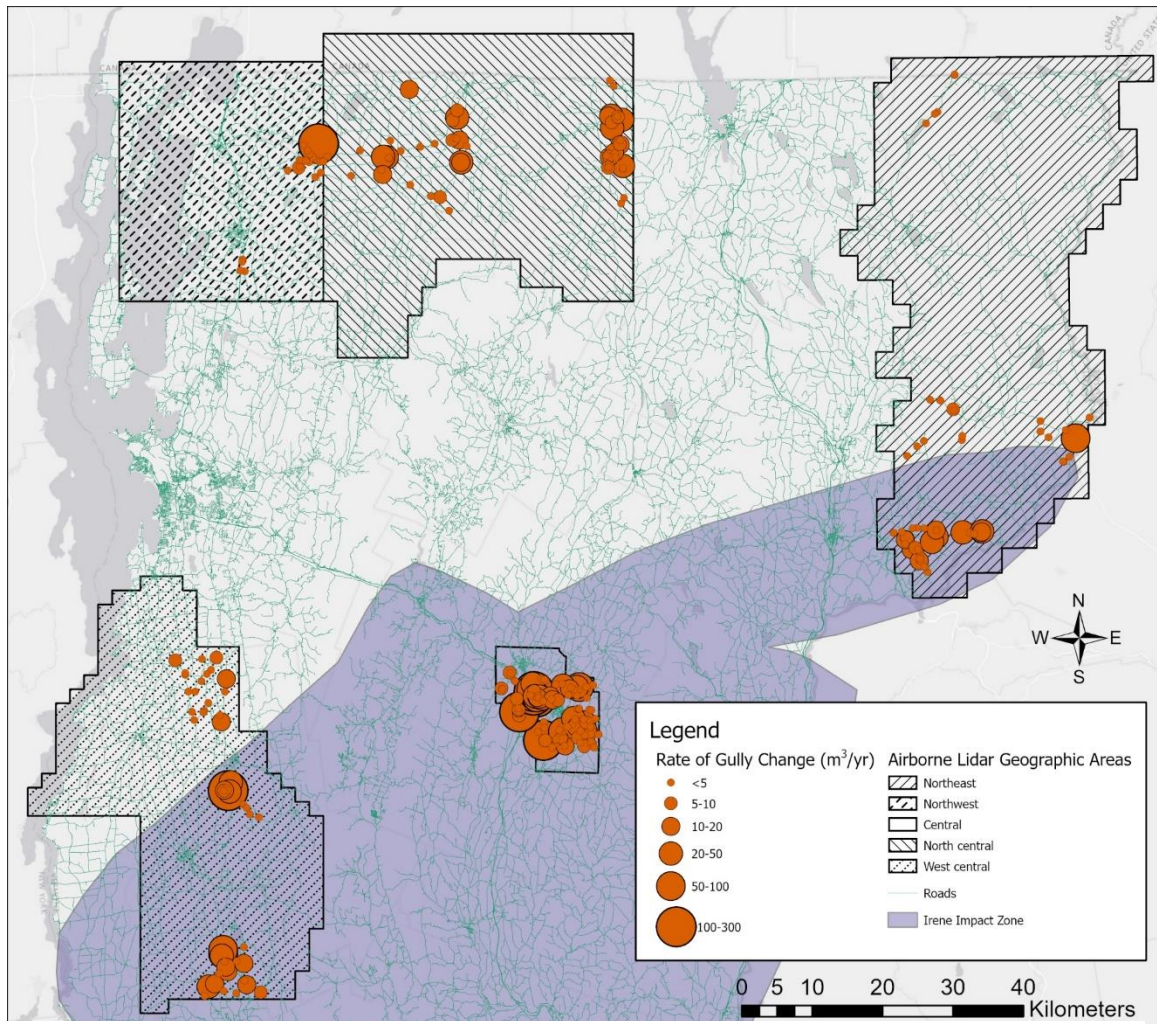


Figure 5. Map showing the spatial distribution of gully volumes over the study area. Each airborne lidar time period is symbolized, and the impact zone of tropical storm Irene is shown. The size of points is based on the rate of gully change where smaller points are less change and larger points are more change. The estimated time periods of each geographic area are northeast 10/31/2005-11/9/2016, northwest 11/7/2008-11/15/2017, central 5/15/2009-11/15/2015, north central 5/15/2010-11/15/2017, and west central 12/7/2012-11/15/2017.

Table 4 describes the uncertainty and resolution of each LiDAR collect. The uncertainty of the DoDs ranged from a standard deviation of 0.099 to 0.155. The mean error among the DoD collects ranged from -0.015 meters to 0.072 meters. The resolution of the DoDs ranged from 1 meter to 1.6 meters which represents the gully detection limits.

Table 4. Uncertainty values associated with the estimates of gully change from the extensive airborne LiDAR work. Resolution of each DoD is also included.

Collect	Resolution (m)	Standard Deviation	Mean Error (m)
Northeast	1	0.155	0.064
Northwest	1.6	0.106	-0.015
Central	1	0.099	0.072
North Central	1.6	0.149	0.061
West Central	1.6	0.114	0.009

3.3.2 Intensive Terrestrial LiDAR Surveys

Gullies studied through our intensive field surveys were located on Interstate highways and on paved and unpaved municipal roads. Sites 1, 2, and 3 drained the road surface and adjacent road margins through a combination of open- and closed-system drainage. Additional sites were paved municipal roads draining closed systems in Winooski, Colchester and Essex, and rural, unpaved class 3 roads draining open systems in Johnson, Stowe and Jericho. Two sites in Stowe (Site 30 and 31) were located on a municipal class 4 road. Surveyed gullies ranged in size from under 2 m³ to over 200 m³ (Table 5).

Table 5. Summary statistics of each of the gullies surveyed. Metrics were calculated from the May 2020 surveys where sites were surveyed within a two-week period.

	Mean	Median	Minimum	Maximum	Range	Total
<i>Gully sites (n=13)</i>						
Contributing Area (m ²)	11,208	6,147	1,490	78,077	76,587	145,701
Volume (m ³)	74.1	60.5	2.0	220.8	218.8	963.4
Length (m)	27.9	29.9	7.9	47.2	39.3	362.8
Maximum width (m)	4.7	5.0	1.5	8.0	6.5	61.5
Maximum depth (m)	1.6	1.7	0.5	3.7	3.2	21.2

Results from the intensive terrestrial LiDAR surveys show that gully volumes are related to characteristics of the sites they drain. Road length, road area, and upslope contributing area explain between 45% and nearly 70% of the variability in gully volume mapped in May 2020 (Figure 6a,b,c). These findings point to the importance of concentrated runoff in scouring gullies at road drainage outfalls. The relationship between larger gullies and steeper slopes at culvert outfalls is not statistically significant (Figure 6d). Site 28 in Middlesex is located on a very steep slope but had the smallest gully volume among the study sites. This site drains a road segment of only 91 m, the third shortest segment among the study sites. Site 2 was located on a low gradient slope but drains a road segment of 323 m and the largest upslope contributing area of all sites.

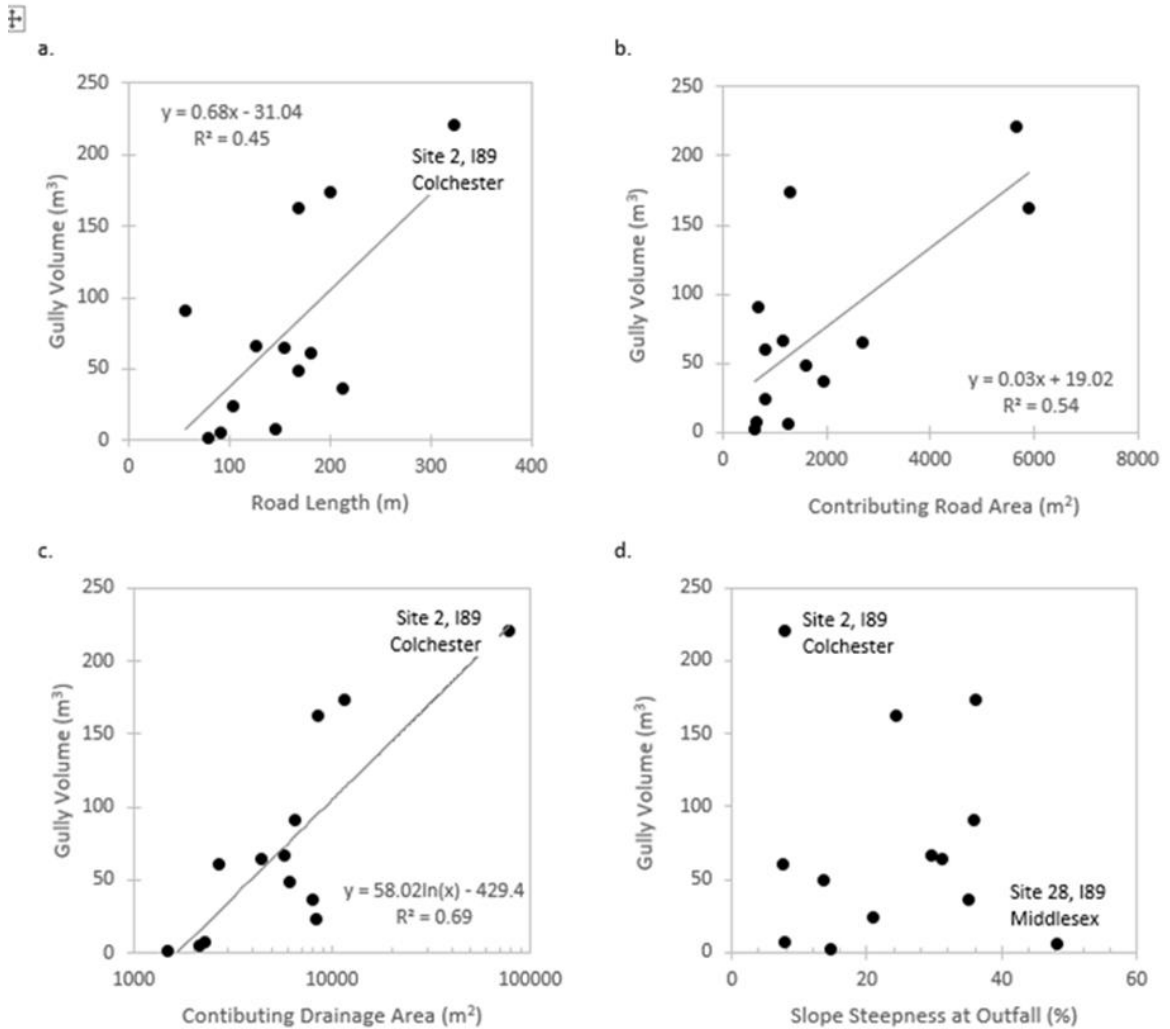


Figure 6. Gully volumes for May 2020 surveys vs. contributing road length (a), contributing road surface area (b), upslope contributing area (c), and slope steepness at culvert outfall (d). Road length, contributing road area, and contributing drainage area all had significant relationships to gully volume and the equation is listed on the graph. Slope steepness did not have a significant relationship to gully volume.

Soil properties appear to exert a lesser influence on gully volume compared to road length and area. Soil erodibility index, taken from NRCS soils data for each site, is statistically related to gully volume, though the form of the relationship is counter intuitive, with higher values of the index (more erodible soils) associated with smaller gully volumes. Mean soil bulk density measured from field samples and soil texture taken from NRCS

soils descriptions also appear less important than contributing water volumes (as indicated by road length, road area, and contributing area) in explaining gully volume.

Repeated surveys of gully sites indicate where changes within the gully occur. Across time periods spanning accumulated rainfall totals ranging from 100 mm to nearly 600 mm, net change of gully volume was generally positive indicating erosion occurred and eroded soils were evacuated from the gully. Instances of negative net gully volume change were also observed, indicating of deposition of soils (possibly from upslope areas) within the gully. The magnitude of change was roughly related to accumulated rainfall totals during the survey intervals (Figure 7). Volume changes of 16 m³ or more occurred at Site 2 and Site 31 for survey intervals with some of the highest accumulated precipitation totals.

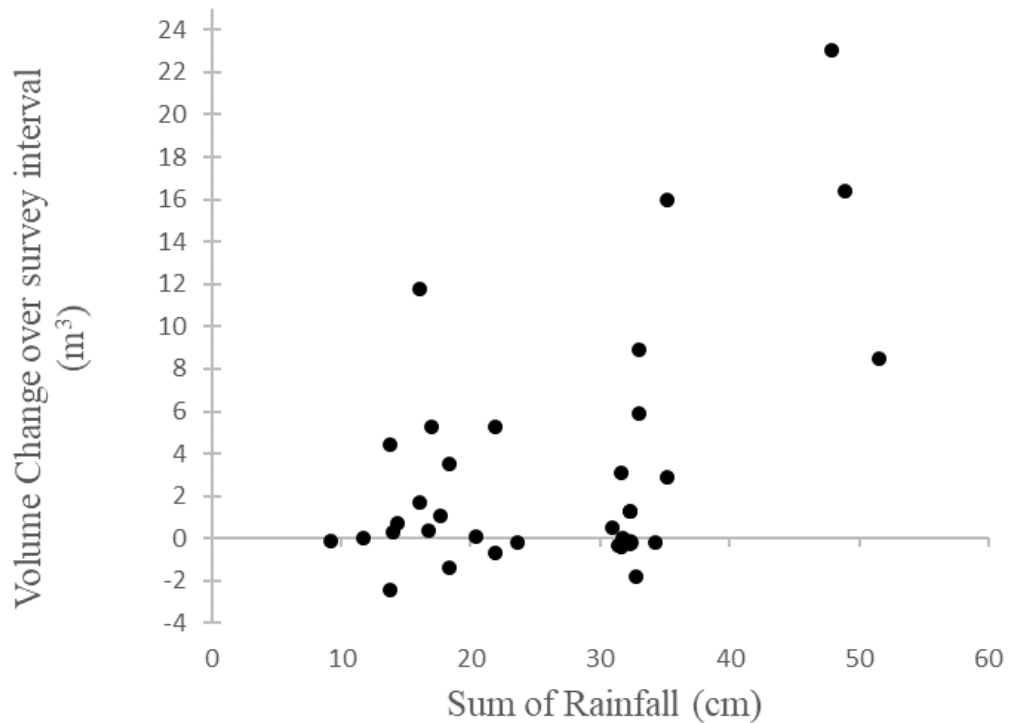


Figure 7. Gully volume change over survey interval and the sum of rainfall to occur during that time. Although there is not a significant relationship between the sum of rainfall and volume change over survey interval. Visually, high rainfalls generally resulted in higher change.

The DEMs shown below show the high level of detail terrestrial LiDAR surveys can produce compared to other field methods (Figure 8). Site 2 shows headcutting erosion above the culvert outlet. Visually, we can see that site 2 has much steeper side slopes compared to site 3. The DEM of difference of site 31 shows the two distinct reaches divided by the downed woody debris. The reach closest to the culvert outlet mostly had deposition occur over the study period with some channel widening occurring in places. The side walls of the gully widen significantly for about 8 m immediately after the downed woody debris. There is some deposition that is seen on the gully floor in these areas as well.

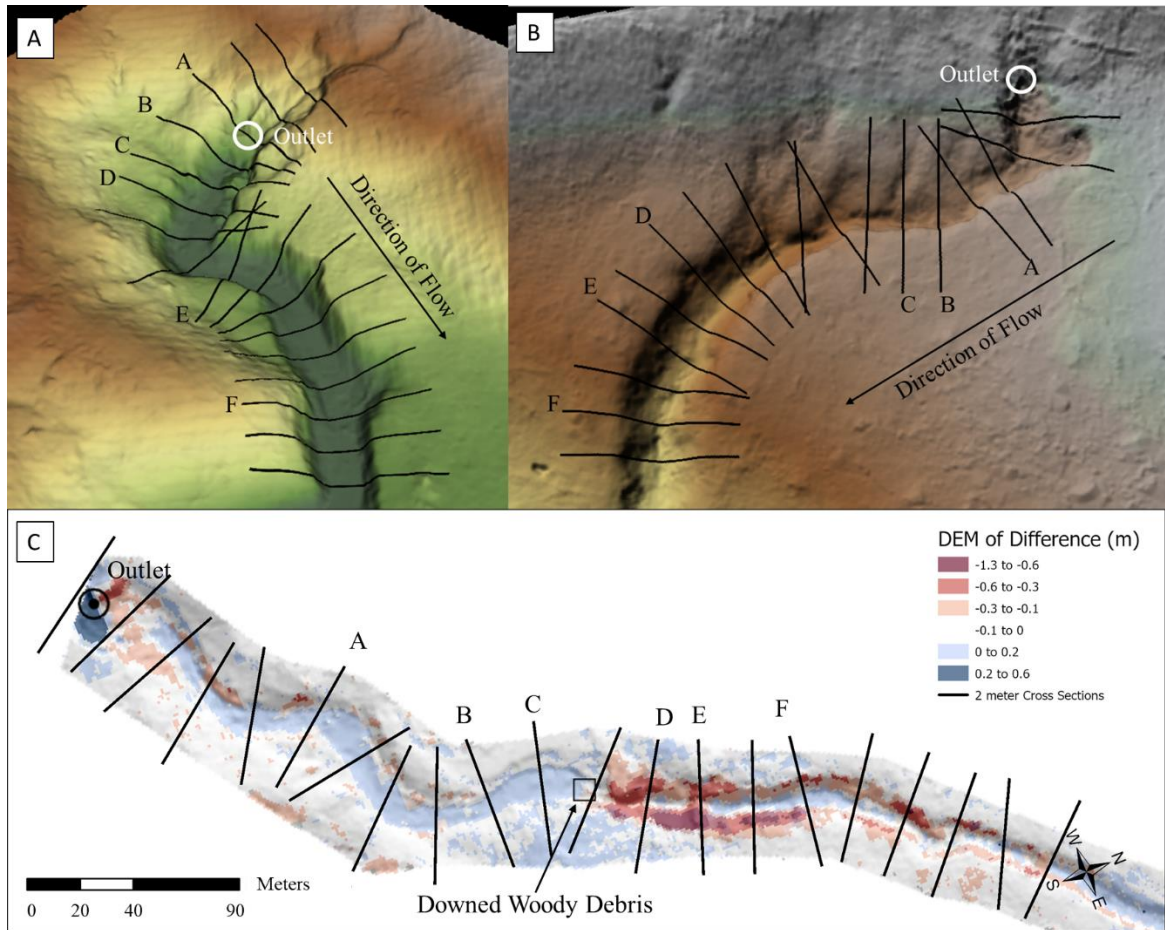


Figure 8. Terrestrial LiDAR scanner derived geospatial products. Each map shows the gully feature of interest, cross sections taken every 2 m, location of culvert outlet, and direction of flow from the culvert. Letters A-F are associated to the cross-section plots in Figure 9. A: Digital elevation model of site 2 with 2-m cross sections. The culvert location is at cross section A, but the gully headcut is located above the culvert outlet. B: Digital elevation model of site 3 with 2 m cross sections. The outlet is in the upper right-hand corner of the figure with the flow of water from the culvert following the gully downslope. C: Digital elevation model of difference of site 31. This shows the elevation change that occurred between the first and last survey of the study period where red cells represent areas of erosion and blue cells represent deposition. The culvert outlet is located in the upper left-hand area of the figure and the flow of water follows the gully moving to the right. This site had woody debris about half way down the gully (symbolized as a black box) which splits this gully into two distinct reaches.

Cross sections extracted from terrestrial LiDAR scans reveal longitudinal patterns of change. The cross sections of site 2 reveal that the greatest magnitude of change occurred by the head cut and beginning of the gully and stabilizes further down the gully

(Figure 9). Downslope gully widening is observed and the side slopes of site 2 are very steep. Site 3 is a relatively stable gully characterized as stage 3. This site has some infilling occurring at cross section B and C where the gully volume decreases. Site 31 has a stark difference of change from before the downed woody debris and after (between C and D). There is deposition occurring in cross sections A, B, and C over the study period. After the downed woody debris, cross sections D and F see widening occurring while E sees a deepening.

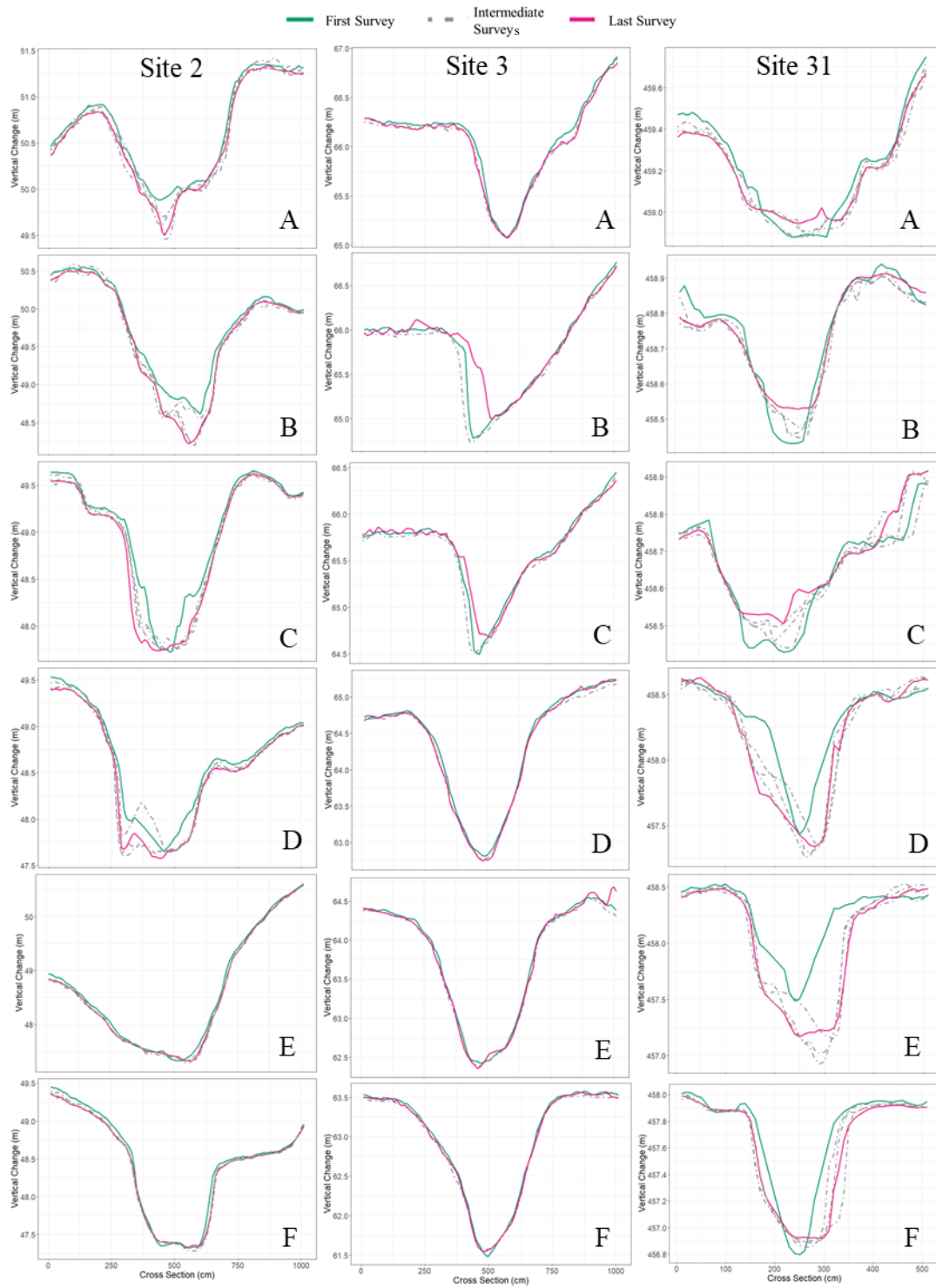


Figure 9. Cross section plots of sites 2, 3, and 31. The label of each cross section is associated to the cross-section labels in Figure 6. The titles are also labeled describing the cross-section position.

Collectively, these high-resolution repeat surveys provide insights into gully evolution for the sites examined. Gully evolution stage and width depth ratios were summarized for a selection of terrestrial LiDAR surveys (Table 6). Site 30 was characterized as stage 1, and it had the highest maximum and mean width/depth ratio. There was very little change at this site over the survey period. Sites 2, 11, and 31 all were characterized as stage 2 which is the most erosional stage in gullies. Sites 2 and 11 were the largest gullies surveyed and site 31 had some of the highest volume change between surveys. Site 11 had the lowest maximum and mean width/depth ratio. Sites 3 and 10 were characterized as stage 3 and overall they had higher width/depth ratios compared to stage 2 gullies. From field observations, sites 3 and 10 had vegetation growing on the gully side slopes which is an indicator of healing within gully systems. Volume changes in stage 3 gullies were lower compared to the stage 2 gullies.

Table 6. Six of the terrestrial LiDAR survey sites were analyzed to assess the gully evolution stage and width/depth ratio. The gully evolution stage was determined by field observations, erosion rate, and morphological changes that occurred over the study period. Width/depth ratios were measured at each 2-meter cross section of the May 2020 survey round. The width and depth were measured from the lower bank of the side slopes to the lowest point in the gully. The width/depth ratio of each cross section was then summarized at the minimum, maximum, and mean ratio.

Site	Gully Stage	Min W/D	Max W/D	Mean W/D
Site 2	2	2.91	5.35	3.90
Site 3	3	2.43	5.65	3.61
Site 10	3	3.04	9.42	4.27
Site 11	2	1.59	2.79	1.87
Site 30	1	4.00	16.25	7.58
Site 31	2 & 4	1.43	7.56	3.68

3.4 Discussion

Results of this study show that gully erosion at road drainage outfalls is a common occurrence, with a frequency of roughly 1 in 10 outfalls exhibiting evidence of gullying among the sites we studied. Gully volume change from the multi-date LiDAR estimations ranged widely, with some of the largest features exceeding 10 m³/yr. Of the volumes estimated, 76% of the features exhibited erosion rates of less than 10 m³/yr. The greatest rates of change occurred on slopes over 20% in the region impacted by Tropical Storm Irene. North central collect did not have any gullies over 50 m³/year and had one of the lowest maximum precipitations which indicates this area had less extreme events compared to other areas.

Both analyses show road length as an important predictor in gullies. Road length, road contributing area, and road drainage area have statistically significant correlations to gully volume which align with results from Seutloali et al (2016). Slope steepness at culvert plays a role in determining gully erosion. There is a positive connection between slope steepness and gully volume which implies that steeper slopes have a greater tendency to gully. There is also evidence that there is interaction between elevation and slope steepness that impacts gully occurrence. From the BRM results there were two peaks of a higher likelihood of gully occurrence at slopes over 20%, one at lower elevations and another at higher elevations. This may be due to impacts from Tropical Storm Irene. The central LiDAR collect had the largest gullies clustered closely to one another on steep slopes.

This study revealed that there is not one singular factor that influences gully occurrence and rates of erosion, and there are complex interactions that influence gully erosion from roads. Some gully erosion processes occur episodically and over a longer time than the two-year study period. The results from the terrestrial LiDAR complement the airborne LiDAR which is over a longer time period than the surveys. The main challenge revealed from the airborne LiDAR analysis is that it is impossible to disentangle the spatial effects (different areas of Vermont) from the different time spans of the LiDAR effects.

It is possible that the gully volume change and cross sections presented in this study are conservative estimates, due to the point density at the bottom of gullies. The underestimation is due to the shape of gullies (side walls and v-shaped cross sections) which makes it difficult to acquire full coverage. Dense vegetation for both airborne and

terrestrial LiDAR is a major error source in estimating volume change (Bremer and Sass 2012).

There are instances of deposition in both the airborne and terrestrial analysis. Well vegetated gully systems are more likely to have deposition occur (Molina et al. 2009). Vegetation on gully walls and side walls less than 45 degrees are indicators of a stabilized gully in stage 3 or 4 (Schumm 1984). Deposition occurrence seen in the airborne LiDAR analysis could be an indicator of gully stabilization.

Overall, we see stabilized gullies (Stage 3 and 4) with higher width/depth ratios compared to stage 2 gullies. Sites 2 and 3 have similar width to depth ratios but were characterized as different gully evolution stages due to the presence of vegetation on site 3 side slopes. Site 3 also saw little change in most of the cross sections, and in some places the gully side wall angles decreased. Site 30 was characterized as stage 1 and has the highest width/depth ratio. Although the width/depth ratio may indicate the gully has stabilized, from field observations we believe this gully is in the channel cutting stage and may eventually move to a stage 2 gully. Stage 1 is when mitigation measures should be implemented (Schumm 1984).

Gully erosion present downstream from culverts in our study at some locations exhibited characteristics of stream channels. The gullies that had characteristics of stream channels often had water flowing during field visits. The distinction between gullies and channels are not always clear cut (Schumm 1984, Bierman 2014). Based on field

observations it seems that the main difference between a stream and a gully is that a stream is in geomorphic equilibrium with its environment and a gully is not.

Although this study did not explicitly focus on mitigating gully erosion from roads, an interesting observation was seen at Site 31 with the downed woody debris. The downed woody debris acted as a check dam to slow down the water flow during storm events enough where larger sediment was deposited in the first reach of the gully. This aligns with other research studying check dams as an effective mitigation measure to increase sediment deposition and reduce lateral bank erosion within gully systems (Alfonso-Torreño et al. 2021). Since road length and contributing drainage areas are an important variable in gully occurrence and rates of erosion, updated road designs could be used to reduce gully formation. A reduction of road contributing area by decreasing drain spacing could reduce gully erosion at culverts, especially where the discharge slopes are steep (Croke and Mockler 2001).

3.5 Conclusions

The application of airborne and terrestrial LiDAR to detect gully occurrence and rates of changes provided new insights into gullies at road drainage outfalls. We found that gullies at road drainage outfalls are a common occurrence in our study region. Median estimate frequency of gully occurrence was one gully every 2 kilometers of road. This study revealed that there is not one singular factor that influences gully occurrence and rates of erosion, and there are complex interactions that influence gully erosion from roads. Their presence seems to be driven by road length, elevation, and slope steepness, revealed by different scales of analysis. Estimates of gully change ranged $-24 \text{ m}^3/\text{year}$ to 269

m³/year with 76% of features examined eroded less than 10m³/year. Many of the largest gullies occurred in areas impacted by Tropical Storm Irene. These features appear to be dynamically evolving, with some evidence that gully stabilization occurs in some sites over time. We infer that gully stabilization may be achieved over time as these features reach an equilibrium slope or when grade controls such as fallen trees arrest incision. This work provides important insights for considering mitigation of gully erosion along transportation networks in this and other settings.

CHAPTER 4: GULLY EROSION AND PHOSPHORUS PRODUCTION

The contents of this chapter previously appeared in the following technical report, published by the Vermont Agency of Transportation, which funded my master’s research project. References to “we” and “our” in this chapter reflect the collaborative nature of the work that went into that technical report:

Wemple, B.C., E. Estabrook, M. Dewoolkar, S. Hamshaw. 2021. Quantifying Nutrient Pollution Reductions Achieved by Erosion Remediation Projects on Vermont’s Roads. Vermont Agency of Transportation Technical Project Report no. 2021-02. Available [here](#)

4.1 Introduction

The results of this study provide a means for estimating the contribution of gully erosion to the production of sediment and sediment-bound phosphorus (P) at the town and watershed level, which may inform P reduction strategies and crediting under the Lake Champlain TMDL. To this end, we provide two examples for “scaling up” the results of the airborne LiDAR data analysis to the town and catchment level to evaluate the importance of this source of phosphorus production, relative to modeled loads. Our approach and estimates are provided below.

4.2 Methods

From the set of 35 towns for which we used airborne LiDAR datasets to identify a larger set of gullies at culvert outlets and estimate change from multi-date LiDAR imagery, we selected five towns to provide an estimate of phosphorus production from gully erosion (Figure 10). For each town, we extracted the set of assessed culverts with gully change estimates (expressed as a volume in m³/yr), multiplied each observation of gully erosional

change by the mean bulk density estimated by Piasecki (2020) and Wemple et al. (2021) ($1,239 \text{ kg/m}^3$) for an estimate of eroded soil mass from gullies per year, and multiplied this quantity by the mean soil phosphorus concentration estimated in this study (694 mg P/kg soil). We then summed this estimate of P production per year for gullies in each town (converting this sum from mg to kg) for a net estimate of phosphorus production, expressed in kg/yr. We repeated this for two HUC12 watersheds, the Missisquoi River from Trout River to Black Creek and Lewis Creek, where we had relatively complete assessments of culvert outlets and estimates of change over time (Figure 11).

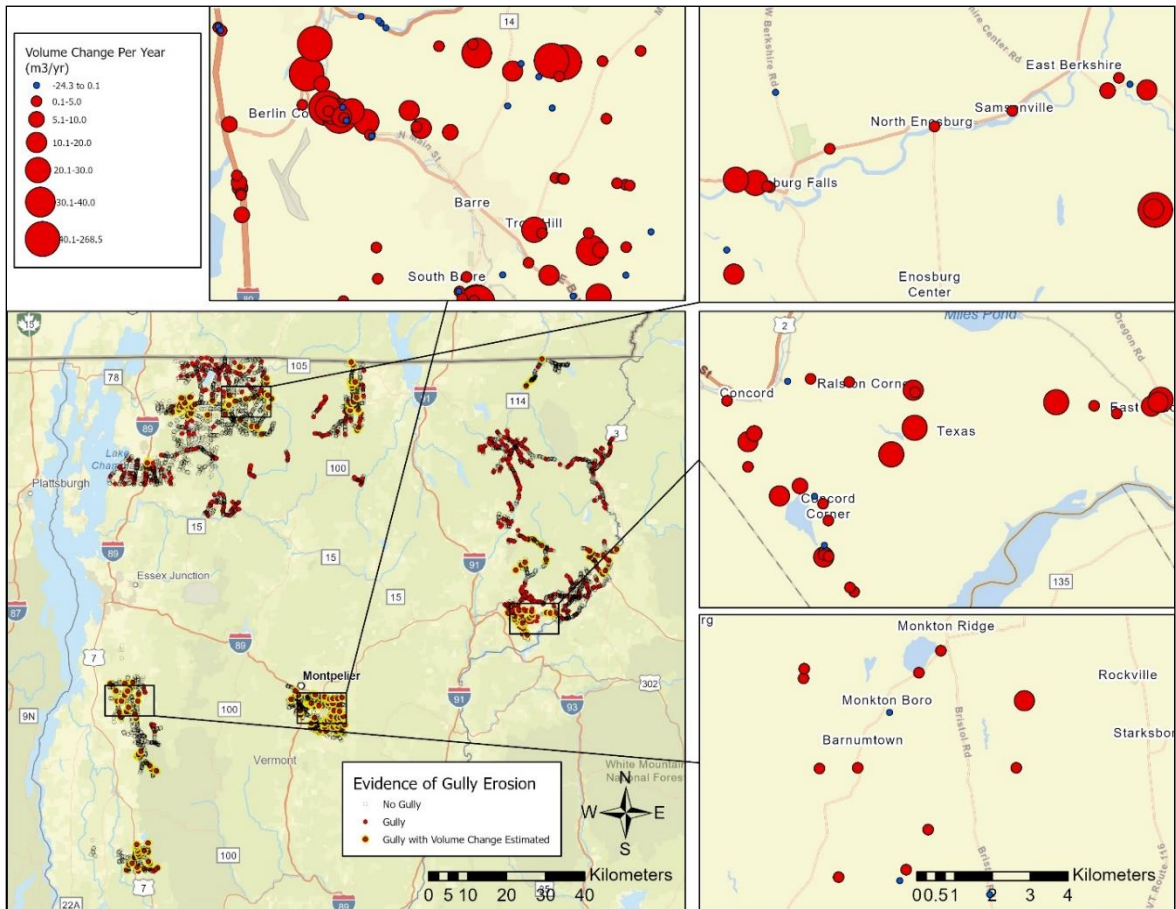


Figure 10. Locations of culverts inspections to assess gully occurrence. Inset panels show selected areas for which gully volume areas were determined by DEM differencing.

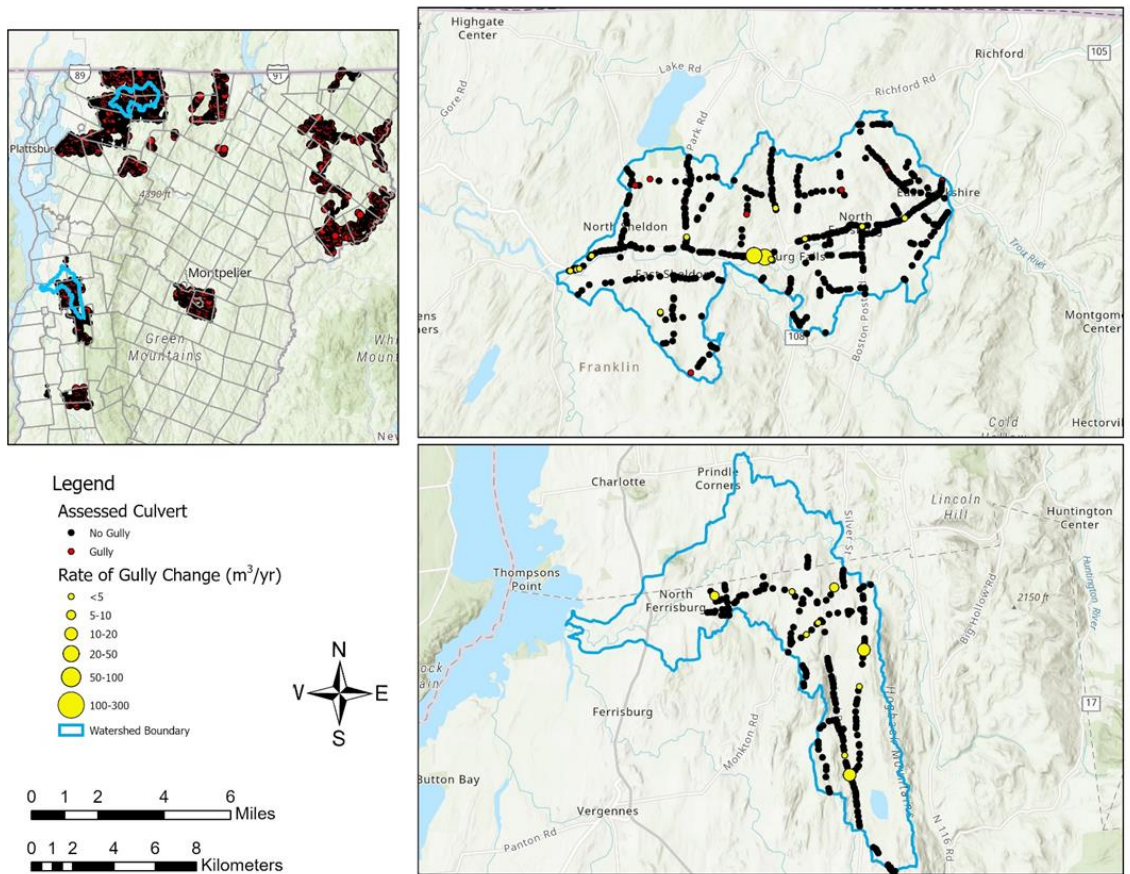


Figure 11. Locations of culvert inspections conducted in GIS to assess gully occurrence (upper left panel, same dataset presented in Figure 10) and detailed maps for two HUC12 watershed where culvert assessments covered much of the watershed.

We referenced this estimate against an estimate of phosphorus loads for each town using the Vermont Clean Water Roadmap tool, available at <https://anrweb.vt.gov/DEC/CWR/CWR-tool>. This tool allows a user to display and interactively identify a HUC12 subwatershed and generate a screen display of total phosphorus (TP) load, expressed in kg/yr. For the town-level analysis, we separately conducted GIS overlays of the town boundaries with the HUC12 watershed boundaries available on the Vermont geodata portal to determine the fraction of town area in each

HUC12 catchment. Using these area proportions, we weighted estimates of HUC12 TP load and summed these area -weighted estimates for a town-level estimate of TP load (see example for Barre town in Table 7).

We note in presenting this analysis that the Clean Water Roadmap tool uses downscaled estimates of TP load from the watershed model used to produce them, introducing some additional uncertainty in these estimates (*Phillip Jones, Vermont Department of Environmental Conservation, personal communication, July 8, 2021*). While the values presented here are clearly a simplification, they provide a first-order estimate of the importance of gully erosion at road drainage outfalls for phosphorus production at the town and subwatershed scale, for a few selected examples.

Table 7. Example of HUC12 subwatersheds covering the town of Barre, with total phosphorus (TP) loads extracted from the Clean Water Roadmap tool. Estimates were weighted for the percentage of town area in each HUC12 subwatershed and summed to generate an estimate of TP load by town.

HUC12 ID from VT subwatershed boundaries_HUC12	HUC12 NAME	Area (m ²)	% Area	TP load from CWR (kg/yr)	HUC12 ID from CWR tool	Weighted TP load (kg/yr)
020100030204	Stevens Branch-Jail Branch to mouth	20,968,910	0.3	5213	41504030103	1478
020100030103	Jail Branch	30,067,528	0.4	4145	41504030102	1649
020100030103	Stevens Branch-headwaters to Jail Branch	23,828,021	0.3	4049	41504030101	1293
total:		79,596,348				4419

4.3 Findings

Using calculations described above for five selected towns, our estimates show that gully erosion at road drainage outfalls comprises a variable share of phosphorus load in the Lake Champlain basin, ranging from quite modest fractions to a more significant fraction, particularly where the frequency of gully erosion on the transportation network is high and gully change in time is on the larger end of estimates we generated (

Table 8). For example, 16 of 19 assessed culverts in Monkton exhibited erosional change over the multi-date LiDAR datasets compared, with a median rate of change of 2.5 m³/yr. The sum of change estimates from these gullies, converted to an estimate of phosphorus production, totals 53 kg/yr. This represents less than 1% of the estimated P load from the subwatersheds draining the town of Monkton. In Berlin, 33 of 42 assessed culverts exhibited erosional change over the multi-date LiDAR datasets compared, with a median change almost three times that in Monkton and a third of the gullies eroding at more than 10 m³/yr. The sum of change estimates from these gullies, converted to an estimate of phosphorus production, totals 1,210 kg/yr, or nearly one-third of the CWR model-estimated phosphorus load for subwatersheds draining the town of Berlin. At the subwatershed scale, for the two cases we generated, gully production of phosphorus represents a small share of the HUC12 modeled load (Table 9).

These estimates are admittedly coarse and miss inclusion of gullies for which we did not have change estimates (Table 8, Table 9) and where our assessments did not cover the full town extents (Figure 10) or HUC12 extents (Figure 11). They also rely on a simplified estimate of town-level or HUC12-scale phosphorus loading, using the CWR tool. Nevertheless, they provide a first order assessment, using the annual gully volumetric change generated by this study, of the relative magnitude of P production associated with erosion at road drainage outfalls and the potential for P reduction with erosion mitigation. Beyond the benefits of mitigating phosphorus pollution, controlling erosion at road drainage outfalls minimizes the transfer to receiving waters of fine sediment, which is a pollutant of concern in many freshwater systems, and secures the integrity of community

investments in valuable transportation infrastructure, making our roadways more resilience to the impacts of extreme storm events and reducing on-going costs of storm damage (Garton 2015, Wemple 2016).

Table 8: Case 1 - summaries for five selected towns used to generate estimates of phosphorus production from gullies and compare to phosphorus load extracted from the Vermont Clean Water Roadmap tool.

	Barre	Berlin	Enosburgh	Monkton	Sheldon
Road length (km)	180.8	101.1	154.6	118.1	116.9
Culverts - Small culvert inventory (no.)	258	626	132	0	212
Culverts - VT culverts (no.)	503	248	459	304	227
Culverts - total (no.)	761	874	591	304	439
Culvert frequency (no./km)	4.2	8.6	3.8	2.6	3.8
Gullies at culvert outlets (no.)	102	48	15	19	33
Percent assessed outlets with gullies	13.4%	5.5%	2.5%	6.3%	7.5%
Gullies with multi-date LiDAR coverage for change assessment	69	42	15	19	25
No. of culverts with net erosional change/yr	56	33	14	16	14
Max. gully change (m ³ /yr)	213.2	268.5	42.8	14.7	100.9
Median gully change (m ³ /yr)	3.4	6.8	4.2	2.5	3.4
No. of eroding gullies with change > 10 m ³ /yr	14	11	5	2	2
Percentage eroding gullies with change > 10 m ³ /yr	25%	33%	36%	13%	14%
Sum - phosphorus production from gullies (kg/yr)	666	1210	110	53	137
HUC 12 phosphorus load (kg/yr)	4419	3802	6174	9188	5640
Gully erosion as percent of HUC12 phosphorus load	15.1%	31.8%	1.8%	0.6%	2.4%

Table 9: Case 2 - summaries for two selected HUC12 subwatersheds used to generate estimates of phosphorus production from gullies and compare to phosphorus load extracted from the Vermont Clean Water Roadmap tool.

	Lewis Creek	Missisquoi Trout River to Black Creek
Road length (km)	152.4	146.1
Culverts - Small culvert inventory (no.)	38	276
Culverts - VT culverts (no.)	661	251
Culverts - total (no.)	699	527
Culvert frequency (no./km)	4.6	3.6
Culverts assessed	226	525
Gullies at culvert outlets (no.)	9	27
Percent assessed outlets with gullies	4.0%	5.1%
Gullies with multi-date LiDAR coverage for change assessment	9	14
No. culverts with net erosional change/yr	8	9
Max. gully change (m ³ /yr)	14.7	29.8
Median gully change (m ³ /yr)	5.2	1.5
No. eroding gullies with change > 10 m ³ /yr	2	2
Percentage eroding gullies with change > 10 m ³ /yr	25%	22%
Sum - phosphorus production from gullies (kg/yr)	40	54
HUC 12 phosphorus load (kg/yr)	6648	10028
Gully erosion as percent of HUC12 phosphorus load	0.6%	0.5%

CHAPTER 5: CONCLUSIONS, REFLECTION AND FUTURE WORK

5.1 Informing Policy

My thesis research aimed to help quantify the rates of sediment and phosphorus production from gully erosion in road settings. As part of the total maximum daily load (TMDL) for phosphorus in Vermont sections of the Lake Champlain Basin, each sector in the state is required to meet certain phosphorus reductions targets. The Vermont Agency of Transportation (VTRANS) is exploring multiple approaches, including addressing storm water production, mitigating erosion at drainage outfalls, and considering opportunities for other phosphorus crediting schemes, including floodplain restoration along road corridors (Underwood et al. 2020). Although, we will only have preliminary data for phosphorus reductions expected from erosion mitigation, I suggest my work to be used to help inform the state on the best way to allocate their resources. I am also hoping my data will assist the state in identifying high priority areas to fix.

My project deliverables will also provide more accurate estimates of sediment and phosphorus loads from gully erosion than the state currently has. With a greater understanding of where gully erosion is likely to occur, some updates to the regulatory guidelines within the Municipal Roads General Permit (MRGP) may be warranted.

Discussions with a technical advisory team convened to advise on the VTRANS project that funded my research revealed a need to identify criteria for “meeting standards” with respect to road drainage outfalls within the VTrans Phosphorus Control Plan and MRGP. The findings of my research can help inform these criteria. The stabilization and treatment of localized erosion from roads provides phosphorus reductions and protects

infrastructure. Translating my research into practice through pollutant reduction credits will help advance the Phosphorus Control Plan under development by the Agency (Macrellis 2020).

I recommend that the state continue to monitor the 13 monitoring sites I have surveyed for this project. Although we have more data and information on gully erosion frequency and rates than before starting the project, a 2-year monitoring period is a short time in the context of assessing geomorphic change. I would encourage the state to consider monitoring sites bi-annually in leaf off conditions (spring and fall) at a minimum to continue our understanding of gully erosion. I am specifically curious if/when a gully stabilizes as that can help the state determine if a large gully is worth the cost of erosion control measures. As part of the MRGP, towns are assessing culvert outlets for erosion and this is an opportunity to also assess change overtime at these outlets. I would also encourage the state to choose a handful of sites that do not yet have gullied but have some features that make them a high risk to gully in the future. It may be worth monitoring these sites to see if they eventually gully. In the future, the state might have enough information to prevent gullying to occur with preventative measures.

Limited funding for implementation of Clean Water projects will undoubtedly constrain the number and extent of gully mitigation projects. Act 76 is the funding and project framework for essential water quality projects to meet Vermont's water quality goals. Although Act 76 seems like a way to streamline funding at the state level, I believe there may be consequences to smaller water quality projects like localized road erosion repair. Results of this study suggest that targeting gullies on steeper slopes (> 20%) and at

higher elevations outside the low gradient terrain of the Champlain valley might be most effective in reducing this source of pollutant delivery to receiving waters. Further targeting mitigation measures on sites that drain longer road segments and discharge to steep slopes may narrow the range of suitable candidates at the local level.

From my research and literature review, I believe available funds should be allocated towards remediating gullies in stage 1 and stage 2 evolution, located on a steeper hillslopes. These gullies have the potential to deliver a large amount of sediment if left untreated and I think in the long term that is more conducive to the TMDL goals.

5.2 Methodological Insights and Challenges

There are three major platform categories for LiDAR: terrestrial, airborne, and UAS. Terrestrial is best for smaller sites that can be accessed easily by car and foot. This is because many terrestrial LiDAR scanners are quite heavy and difficult to carry long distances. Terrestrial scanners are best suited for sites that have vertical facing structures like rock slopes or gully walls (Bremer and Sass 2012). Terrestrial LiDAR can be used quickly and would be good for sites with multi-temporal surveys (<1 survey per month). Airborne LiDAR scans are best suited for very large areas where it is not feasible to conduct a terrestrial or UAS scan. Since airborne LiDAR scans are installed on manned aircrafts, this platform has the most acquisition logistics to figure out and this route may be best suited for projects where a researcher is only look for a few acquisitions (pre- and post-analysis). Airborne LiDAR in general has lower resolution than terrestrial or UAS scans. UAS LiDAR scanners are best for small to medium sized sites that may be more difficult to access. UAS and Airborne LiDAR are best suited for horizontal structures (Bremer and

Sass 2012). UAS LiDAR can be used quickly and would be best suited for sites with multi-temporal and hyper-temporal surveys. A UAS can be used by the researcher in the field, but whoever is piloting the UAS must have their Part 107 Remote Pilot License to adhere to federal law. UAS also have specific airspace rules pilots must follow so the site location should be reviewed for airspace prior to field work.

There are some significant potential challenges that should be considered when undertaking an intensive LiDAR survey approach of the type completed for this study. A terrestrial LiDAR scanner has a limited field of view since it is on the ground where vegetation and tree trunks can block the view to the gully of interest. Large data files are also another potential challenge that should be considered. Single project files for this project ranged from 6 – 21 GB. With multiple surveys for many sites, the size of files adds up quickly and ample data storage best practices should be considered. Challenges in dataset size has also been discussed in the literature when expanding the temporal dimensions of LiDAR data (Eitel et al. 2016). The topography and access of the landscape of interest may pose a potential challenge.

Two key challenges exist when employing multi-date LiDAR: registration of multiple datasets for one site and time demands of data processing. Multi-temporal LiDAR surveys have additional processing steps to ensure the datasets are registered correctly. For projects only using one LiDAR platform (terrestrial vs airborne), it is more straightforward than projects using terrestrial and airborne LiDAR to monitor change. Processing the terrestrial LiDAR point clouds for the gully erosion study is time consuming where one survey can take 8-12 hours to estimate the gully volume. Due to the distinct qualities of

airborne and terrestrial LiDAR point clouds, the alignment and filtering processing steps required to ensure the datasets line up are even more time consuming. A case study in Austria required several months of processing to estimate landscape change (Bremer and Sass 2012).

Interpreting results from multiple LiDAR platforms adds to the potential challenges because of the different characteristics of the point clouds. In a study by Perroy et al (2010), researchers monitoring gully volume estimates through airborne and ground-based LiDAR found that both methods underestimated erosion volumes because of an overestimated gully bottom surface area. Due to the shape of gullies (typically V-shaped) it poses a unique challenge to acquire a high point density at the bottoms of gullies. The researcher concluded that LiDAR can be used to quantify gully volumes, great care must be taken to increase accuracy. Dense vegetation cover has also been documented as a serious error source in both terrestrial and airborne LiDAR (Bremer and Sass 2012).

The following is a set of recommendations a researcher should consider when utilizing LiDAR surveying to monitor landscape change. The most important consideration to make is if LiDAR is an appropriate field method for a project. LiDAR is best for projects that need a high level of resolution and accuracy. If LiDAR is determined to be the best method, then the LiDAR scanner type and platform to be used for field work should be decided on. A researcher must also have a clear idea on the type(s) of landscape they will conduct the surveys at as the landscape of interest will determine what LiDAR system is best. Some questions to ask: How large of an area am I planning on surveying? How often do I want to survey to track change? What kind of spatial resolution do I need? Is the area

densely vegetated or within a forest? Ease of access to landscape of interest? When determining how often a survey should occur, the rate of geomorphic change should decide the survey recurrence interval. Hyper-temporal (>1 survey per month) surveys are often needed to completely capture geomorphic change (Eitel et al. 2016).

As LiDAR technology advances, it offers increased opportunities for monitoring environmental change. As Vermont begins to have multiple time periods of statewide LiDAR data products, there is opportunity to create DEMs of difference that could track erosional change on slopes and in river corridors.

LITERATURE CITED

- Alfonso-Torreño, A., Á. Gómez-Gutiérrez, and S. Schnabel. 2021. Dynamics of Erosion and Deposition in a Partially Restored Valley-Bottom Gully. *Land* **10**:62.
- Arabameri, A., B. Pradhan, H. R. Pourghasemi, K. Rezaei, and N. Kerle. 2018. Spatial modelling of gully erosion using GIS and R programming: A comparison among three data mining algorithms. *Applied sciences* **8**:1369.
- Bierman, P. R. a. 2014. Key concepts in geomorphology. New York, NY : W.H. Freeman and Company Publishers : A Macmillan Higher Education Company.
- Blanton, P., and W. A. Marcus. 2009. Railroads, roads and lateral disconnection in the river landscapes of the continental United States. *Geomorphology* **112**:212-227.
- Bremer, M., and O. Sass. 2012. Combining airborne and terrestrial laser scanning for quantifying erosion and deposition by a debris flow event. **138**:49-60.
- Bretherton, S. 1972. Stability and the conservation of mass in drainage basin evolution. *Water Resources Research* **8**.
- Bull, L., and M. Kirkby. 1997. Gully processes and modelling. *J Progress in Physical Geography* **21**:354-374.
- Buston, P. M., and J. Elith. 2011. Determinants of reproductive success in dominant pairs of clownfish: a boosted regression tree analysis. *Journal of Animal Ecology* **80**:528-538.
- Castillo, C., and J. A. Gómez. 2016. A century of gully erosion research: Urgency, complexity and study approaches. *Earth-Science Reviews* **160**:300-319.
- Castillo, C., R. Perez, M. R. James, J. N. Quinton, E. V. Taguas, and J. A. Gomez. 2012. Comparing the Accuracy of Several Field Methods for Measuring Gully Erosion. *Soil Science Society of America Journal* **76**:1319-1332.
- Castle, S. S., E. A. Howe, E. L. Bird, and W. G. Howland. 2013. Flood Resilience in the Lake Champlain Basin and Upper Richelieu River. *Lake Champlain Basin Program*.
- Conforti, M., P. P. C. Aucelli, G. Robustelli, and F. Scarciglia. 2011. Geomorphology and GIS analysis for mapping gully erosion susceptibility in the Turbolo stream catchment (Northern Calabria, Italy). *Natural Hazards* **56**:881-898.
- Croke, J., and S. Mockler. 2001. Gully initiation and road-to-stream linkage in a forested catchment, southeastern Australia. *Earth Surface Processes and Landforms* **26**:205-217.
- Daba, S., W. Rieger, and P. Strauss. 2003. Assessment of gully erosion in eastern Ethiopia using photogrammetric techniques. *CATENA* **50**:273-291.
- E.P.A. 2016. Phosphorus TMDLs for Vermont Segments of Lake Champlain.
- Eitel, J. U., B. Höfle, L. A. Vierling, A. Abellán, G. P. Asner, J. S. Deems, C. L. Glennie, P. C. Joerg, A. L. LeWinter, and T. S. Magney. 2016. Beyond 3-D: The new spectrum of lidar applications for earth and ecological sciences. *Geomorphology* **186**:372-392.
- Elith, J., J. R. Leathwick, and T. Hastie. 2008. A working guide to boosted regression trees. *Journal of Animal Ecology* **77**:802-813.

- Forman, R. T., D. Sperling, J. A. Bissonette, A. P. Clevenger, C. D. Cutshall, V. H. Dale, L. Fahrig, R. L. France, C. R. Goldman, and K. Heanue. 2003. Road ecology: science and solutions. Island press.
- Frankl, A., J. Poesen, M. Haile, J. Deckers, and J. Nyssen. 2013. Quantifying long-term changes in gully networks and volumes in dryland environments: The case of Northern Ethiopia. *Geomorphology* **201**:254-263.
- Galia, T., K. Silhan, and V. Skarpich. 2017. The geomorphic impacts of culverts at paved forest roads: Examples from Carpathian headwater channels, Czech Republic. *CATENA* **157**:424-435.
- Garton, J. S. 2015. Master's Project: Evaluating the Effectiveness of Best Management Practices on Rural Backroads of Vermont: A Retrospective Assessment and Cost Analysis. Rubenstein School Masters Project Publications.
- Grayson, R., S. Haydon, M. Jayasuriya, and B. Finlayson. 1993. Water quality in mountain ash forests—separating the impacts of roads from those of logging operations. *Journal of Hydrology* **150**:459-480.
- Hamshaw, S. D., T. Bryce, D. M. Rizzo, J. O'Neil-Dunne, J. Frolik, M. M. J. R. r. Dewoolkar, and applications. 2017. Quantifying streambank movement and topography using unmanned aircraft system photogrammetry with comparison to terrestrial laser scanning. **33**:1354-1367.
- Hayas, A., A. Peña, and T. Vanwalleghem. 2019. Predicting gully width and widening rates from upstream contribution area and rainfall: A case study in SW Spain. *Geomorphology* **341**:130-139.
- Heidemann, H. K. 2012. Lidar base specification. 2328-7055, US Geological Survey.
- Ireland, H. A., D. H. Eargle, and C. F. S. Sharpe. 1939. Principles of gully erosion in the Piedmont of South Carolina. US Department of Agriculture.
- Jones, J. A., F. J. Swanson, B. C. Wemple, and K. U. Snyder. 2000. Effects of roads on hydrology, geomorphology, and disturbance patches in stream networks. *Conservation Biology* **14**:76-85.
- Junior, O. C., R. Guimaraes, L. Freitas, D. Gomes-Loebmann, R. A. Gomes, E. Martins, and D. R. Montgomery. 2010. Urbanization impacts upon catchment hydrology and gully development using mutli-temporal digital elevation data analysis. *Earth Surface Processes and Landforms: The Journal of the British Geomorphological Research Group* **35**:611-617.
- Katz, H. A., J. M. Daniels, and S. Ryan. 2014a. Slope-area thresholds of road-induced gully erosion and consequent hillslope–channel interactions. *Earth Surface Processes and Landforms* **39**:285-295.
- Katz, H. A., J. M. Daniels, and S. Ryan. 2014b. Slope-area thresholds of road-induced gully erosion and consequent hillslope–channel interactions. *Earth Surface Processes and Landforms* **39**:285-295.
- Kirkby, M., and L. Bracken. 2009. Gully processes and gully dynamics. *Earth Surface Processes Landforms: The Journal of the British Geomorphological Research Group* **34**:1841-1851.
- Macrellis, A. 2020. Lake Champlain Basin Generalized Phosphorus Control Plan for the Vermont Agency of Transportation. Stone Environmental.

- Martin, T. 2016. The Vermont Clean Water Act: Water Quality Protection, Land use, and the Legacy of Tropical Storm Irene. *Vermont Journal of Environmental Law* **17**:408.
- Mears, D., and T. Martin. 2016. Foreward: Restoring and Maintaining the Ecological Integrity of Lake Champlain. *Vermont Journal of Environmental Law* **17**:408.
- Molina, A., G. Govers, F. Cisneros, and V. Vanacker. 2009. Vegetation and topographic controls on sediment deposition and storage on gully beds in a degraded mountain area. *Earth Surface Processes and Landforms* **34**:755-767.
- Montgomery, D. R. 1994. Road surface drainage, channel initiation, and slope instability. *Water Resources Research* **30**:1925-1932.
- Montgomery, D. R., and W. E. J. N. Dietrich. 1988. Where do channels begin? **336**:232-234.
- Perroy, R. L., B. Bookhagen, G. P. Asner, and O. A. Chadwick. 2010. Comparison of gully erosion estimates using airborne and ground-based LiDAR on Santa Cruz Island, California. *Geomorphology* **118**:288-300.
- Piasecki, F. C. 2020. Quantifying and Predicting Gully Erosion and its Contribution to Nutrient Pollution from Vermont's Roads. University of Vermont Undergraduate Thesis:1-37.
- Poesen, J. 2011. Challenges in gully erosion research. *Landform analysis* **17**:5-9.
- Poesen, J., J. Nachtergaele, G. Verstraeten, and C. Valentin. 2003. Gully erosion and environmental change: importance and research needs. *CATENA* **50**:91-133.
- Ritter, D. F., R. C. Kochel, and J. R. Miller. 2002. Process geomorphology.
- Schumm, S. A. 1984. Incised channels : morphology, dynamics, and control. Littleton, Colo. : Water Resources Publications, Littleton, Colo.
- Seutloali, K. E., and H. R. Beckedahl. 2015. A review of road-related soil erosion: an assessment of causes, evaluation techniques and available control measures. *Earth Sciences Research Journal* **19**:73-80.
- Seutloali, K. E., H. R. Beckedahl, T. Dube, and M. Sibanda. 2016. An assessment of gully erosion along major armoured roads in south-eastern region of South Africa: a remote sensing and GIS approach. *Geocarto International* **31**:225-239.
- Smeltzer, E. 2016. History of Vermont's Lake Champlains Phosphorus Reduction Efforts. *Vermont Journal of Environmental Law* **17**:408.
- Tetra Tech, I. 2015. Lake Champlain Basin SWAT Model Configuration, Calibration and Validation.
- Underwood, K., L. Worley, S. Drago, M. Dewoolkar, D. Rizzo, A. Bomblies, and B. Wemple. 2020. Evaluating effectiveness of floodplain reconnection sites along the Lamoille Valley rail trail: A blueprint for future rail-river projects. Vermont Agency of Transportation
- USDA-SCS, U. S. D. o. A. S. C. S. 1966. Procedure for Determining Rates of Land Damage, Land Depreciation, and Volume of Sediment Produced by Gully Erosion. Technical Release **No. 32**.
- Wemple. 2016. Controlling polluted stormwater runoff from roads. *Vermont Journal of Environmental Law* **17**:785-810.

- Wemple, B. C., G. E. Clark, D. S. Ross, and D. M. Rizzo. 2017. Identifying the spatial pattern and importance of hydro-geomorphic drainage impairments on unpaved roads in the northeastern USA. *Earth Surface Processes and Landforms* **42**:1652-1665.
- Wemple, B. C., J. A. Jones, and G. E. Grant. 1996. Channel network extension by logging roads in two basins, western Cascades, Oregon. *Water Resources Bulletin* **32**:1195-1207.
- Winslow, M. 2015. A Natural and Human History of Lake Champlain. *Vt. J. Envtl. L.* **17**:482.